Journal of Statistical Mechanics:
Theory and Experiment

PAPER

Statistics of diffusive encounters with a small target: three complementary approaches

Journal of Statistical Mechanics: Theory and Experiment
An IOP and SISSA journal

PAPER: Classical statistical mechanics, equilibrium and non-equilibrium

Statistics of diffusive encounters with a small target: three complementary approaches

Denis S Grebenkov*

Laboratoire de Physique de la Matière Condensée (UMR 7643), CNRS—Ecole Polytechnique, IP Paris, 91128 Palaiseau, France
Institute for Physics and Astronomy, University of Potsdam, 14476 Potsdam-Golm, Germany
E-mail: denis.grebenkov@polytechnique.edu

Received 13 May 2022
Accepted for publication 22 July 2022
Published 24 August 2022

Online at stacks.iop.org/JSTAT/2022/083205
https://doi.org/10.1088/1742-5468/ac85ec

Abstract. Diffusive search for a static target is a common problem in statistical physics with numerous applications in chemistry and biology. We look at this problem from a different perspective and investigate the statistics of encounters between the diffusing particle and the target. While an exact solution of this problem was recently derived in the form of a spectral expansion over the eigenbasis of the Dirichlet-to-Neumann operator, the latter is generally difficult to access for an arbitrary target. In this paper, we present three complementary approaches to approximate the probability density of the rescaled number of encounters with a small target in a bounded confining domain. In particular, we derive a simple fully explicit approximation, which depends only on a few geometric characteristics such as the surface area and the harmonic capacity of the target, and the volume of the confining domain. We discuss the advantages and limitations of three approaches and check their accuracy. We also deduce an explicit approximation for the distribution of the first-crossing time, at which the number of encounters exceeds a prescribed threshold. Its relations to common first-passage time problems are discussed.

Keywords: Brownian motion, chemical kinetics, diffusion, first passage

*Author to whom any correspondence should be addressed.

1742-5468/22/083205+34$33.00

Contents

1. Introduction

Various aspects of the first-passage problem for perfect and partially reactive targets have been intensively studied over the past two decades [1–22]. A somewhat related but poorer understood problem is the statistics of encounters of a diffusing particle with a target. How many times does the particle meet the target? Conventionally, the statistics of encounters and the related first-encounter times were studied for two (or many) mobile particles that can represent, e.g. a protein and its receptor, or a prey and its predator [23–37]. In turn, we are interested here in the number of encounters of a diffusing particle with a static target up to time t. For a random walk on a lattice or a graph, this is the random number of visits of a given target site (or a group of such sites) up to time t. For continuous diffusion, this number can be related to the residence time of Brownian motion in a given subset of a confining domain. Alternatively, one can consider the target located on an impenetrable boundary (figure 1), and the number of encounters is directly related to the so-called boundary local time ℓ_t on that region up to time t [38–41]. As explained below, the random variable ℓ_t can be defined as a rescaled residence time in a thin boundary layer near the target, or as a rescaled number of downcrossings (encounters) of that layer. The statistics of such encounters was recently shown to be tightly related to the survival probability on a partially reactive

J. Stat. Mech. (2022) 083205

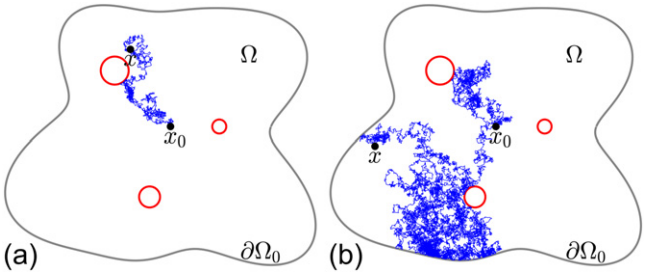

Figure 1. Schematic illustration of a random trajectory (in blue) of a particle that started from $\boldsymbol{x}_0$ and diffused inside a confining domain Ω delimited by a reflecting boundary $\partial\Omega_0$ (in gray) towards small targets (in red). (a) At short times, the particle typically encounters either none, or one target. (b) At long times, the particle can encounter many targets or realize several 'long-range returns' to the same target.

target [42, 43]; it can therefore be viewed as a complementary insight onto the latter problem. Moreover, the knowledge of this statistics allows one to investigate much more general surface-reaction mechanisms, for instance, those with encounter-dependent reactivity [43], which go far beyond the common setting of partially reactive targets [44–62]. A general spectral representation of the distribution of encounters and several explicit examples have been studied within the so-called encounter-based approach [63–67]. However, to our knowledge, this problem has not been addressed in the common case of a *small* target surrounded by an outer reflecting boundary of a confining domain.

In this paper, we employ three recently developed approximations to study the statistics of diffusive encounters with a small target (or multiple targets). In section 2, we formulate the problem and recall the definition of the boundary local time as a proxy of the number of encounters. We also summarize the theoretical ground needed to describe the statistics of encounters and its relation to diffusion-controlled reactions. Section 3 presents three complementary approaches to deal with small targets. The first approach is the matched asymptotic analysis (MAA), which was systematically employed over the past three decades to investigate various first-passage times [68–77] (see also a review [78]). Recently, Bressloff extended this method to the encounter-based description of diffusion-mediated surface phenomena and derived the asymptotic expansion of the so-called full propagator [79]. In section 3.1, we apply his asymptotic results to get the statistics of diffusive encounters and discuss advantages and limitations of this powerful method. The second approach relies on an explicit approximation for the principal eigenvalue of the Laplace operator in the presence of a small partially reactive target [80]. The smallness of the target also ensures that the principal eigenmode provides the dominant contribution to the volume-averaged survival probability, from which the distribution of encounters will be deduced in a fully explicit way (section 3.2). The derived approximation in equation (58) is one of the main results of the paper. The third approach is based on the self-consistent approximation (SCA), which was originally proposed for computing reaction rates [81] and then extended for the analysis of first-passage times [82–86]. We employ its most general form given in [86] to deduce an approximate spectral representation for the distribution of diffusive encounters (section 3.3). This

J. Stat. Mech. (2022) 083205

formal representation clarifies some general properties of the distribution. Moreover, in some symmetric domains such as a spherical target surrounded by a larger concentric reflecting sphere, the SCA turns out to be exact and can thus serve as a benchmark for accessing the quality of two other approximations. We choose this geometric setting to illustrate the accuracy of different approaches in section 4. In section 5, we obtain an explicit approximation (90) for the probability density of the first-crossing time of a given threshold ℓ by ℓ_t. Section 6 summarizes the main findings of the paper, their applications and future perspectives.

2. Boundary local time

We consider a point-like particle that undergoes reflected Brownian motion with a constant diffusivity D inside an Euclidean domain $\Omega \subset \mathbb{R}^d$ with a smooth bounded impermeable boundary $\partial\Omega$. The particle starts from a point $\boldsymbol{x}_0 \in \Omega$ at time 0, and its random position at time t is denoted as $\mathbf{X}_t$. We are interested in the statistics of encounters of the particle with a subset Γ of the boundary that we call a target. If the subset Γ is not connected, one can speak about multiple (disconnected) targets. For the sake of clarity, we mainly speak about a connected (single) target, even though our results are applicable to multiple targets if they are located sufficiently far away from each other (see below). The remaining part of the boundary, $\partial\Omega_0 = \partial\Omega \setminus \Gamma$, ensures normal reflections that confine the particle inside Ω. Following Lévy's construction [38], we introduce the boundary local time ℓ_t spent *on the target* up to time t. This is a stochastic process that can be understood as the renormalized residence time of $\mathbf{X}_t$ in a thin layer of width a near the target, $\Gamma_a = \{\boldsymbol{x} \in \Omega : |\boldsymbol{x} - \Gamma| < a\}$, up time t [39, 40]:

$$\ell_t = \lim_{a\to 0} \frac{D}{a} \underbrace{\int_0^t \mathrm{d}t' \, \mathbb{I}_{\Gamma_a}(\mathbf{X}_{t'})}_{\text{residence time in } \Gamma_a}, \tag{1}$$

where $\mathbb{I}_{\Gamma_a}(\boldsymbol{x})$ is the indicator function of Γ_a: $\mathbb{I}_{\Gamma_a}(\boldsymbol{x}) = 1$ if $\boldsymbol{x} \in \Gamma_a$, and 0 otherwise. This relation highlights that the residence time in the layer Γ_a vanishes in the limit $a \to 0$ when Γ_a shrinks to the target Γ. This is not surprising given that the boundary $\partial\Omega$ has a lower dimension, $d-1$, as compared to the dimension d of the domain Ω, and the residence time on the boundary or any of its subsets is strictly zero. In turn, the rescaling of the residence time in the layer Γ_a by its width a yields a well-defined limit—the boundary local time. Importantly, equation (1) implies that the residence time in a thin layer Γ_a can be approximated as $a\ell_t/D$, as soon as a is small enough. The boundary local time ℓ_t is thus the proper intrinsic characteristics of reflected Brownian motion on the target, which is independent of the layer width used. Note that ℓ_t has units of length, while ℓ_t/D has units of time per length.

The boundary local time ℓ_t is also related to the number $\mathcal{N}_t^a$ of downcrossings of the boundary layer Γ_a by reflected Brownian motion up to time t, multiplied by a, in the limit $a \to 0$ [39, 40]:

$$\ell_t = \lim_{a\to 0} a\mathcal{N}_t^a. \tag{2}$$

J. Stat. Mech. (2022) 083205

The number of downcrossings can thus be interpreted as the number of encounters of the particle with the target. Expectedly, this number diverges in the limit $a \to 0$, because Brownian motion is known to hit a smooth boundary an infinite number of times during any time period after the first hit [87]. A finite thickness a of the layer is needed here to overcome this problem and to get a proper definition for the number of encounters (see further discussions in [42, 43]). As previously, ℓ_t/a is a good proxy for the number of encounters when a is small enough. In the following, we focus on the boundary local time ℓ_t, sometimes referring to it as the rescaled number of encounters.

The boundary local time plays the central role in the encounter-based approach to surface-mediated diffusion phenomena [42, 43, 63–67]. In particular, the joint distribution of the particle position $\mathbf{X}_t$ and its boundary local time ℓ_t is characterized by the joint probability density $P(\boldsymbol{x}, \ell, t|\boldsymbol{x}_0)$ that was called the full propagator. The integral of $P(\boldsymbol{x}, \ell, t|\boldsymbol{x}_0)$ over the arrival point $\boldsymbol{x}$ yields the (marginal) probability density of the boundary local time ℓ_t:

$$\rho(\ell, t|\boldsymbol{x}_0) = \int\limits_{\Omega} \mathrm{d}\boldsymbol{x}\, P(\boldsymbol{x}, \ell, t|\boldsymbol{x}_0). \tag{3}$$

In turn, the Laplace transform of $P(\boldsymbol{x}, \ell, t|\boldsymbol{x}_0)$ with respect to ℓ was shown to determine the conventional propagator $G_q(\boldsymbol{x}, t|\boldsymbol{x}_0)$ in the presence of a partially reactive target [43]:

$$G_q(\boldsymbol{x}, t|\boldsymbol{x}_0) = \int\limits_0^{\infty} \mathrm{d}\ell\, \mathrm{e}^{-q\ell} P(\boldsymbol{x}, \ell, t|\boldsymbol{x}_0). \tag{4}$$

The latter satisfies the diffusion equation

$$\partial_t G_q(\boldsymbol{x}, t|\boldsymbol{x}_0) = D\Delta G_q(\boldsymbol{x}, t|\boldsymbol{x}_0) \quad (\boldsymbol{x} \in \Omega), \tag{5}$$

subject to the initial condition $G_q(\boldsymbol{x}, 0|\boldsymbol{x}_0) = \delta(\boldsymbol{x} - \boldsymbol{x}_0)$ with a Dirac distribution $\delta(\boldsymbol{x} - \boldsymbol{x}_0)$, and mixed Robin–Neumann boundary condition:

$$\partial_n G_q(\boldsymbol{x}, t|\boldsymbol{x}_0) + qG_q(\boldsymbol{x}, t|\boldsymbol{x}_0) = 0 \quad (\boldsymbol{x} \in \Gamma), \tag{6a}$$

$$\partial_n G_q(\boldsymbol{x}, t|\boldsymbol{x}_0) = 0 \quad (\boldsymbol{x} \in \partial\Omega_0), \tag{6b}$$

where Δ is the Laplace operator, and ∂_n is the normal derivative oriented outwards the domain Ω. This condition claims that the diffusive flux $-D\partial_n G_q(\boldsymbol{x}, t|\boldsymbol{x}_0)$ vanishes on the impermeable part of the boundary, $\partial\Omega_0$; in turn, on the target Γ, the diffusive flux is equal to the reaction flux, given by $\kappa G_q(\boldsymbol{x}, t|\boldsymbol{x}_0)$, with a reactivity $\kappa = qD$. In this way, the parameter q of the Laplace transform in equation (4) naturally re-appears in the Robin boundary condition (6a). Expectedly, q can vary between 0 for an inert target with Neumann boundary condition ($\partial_n G_0(\boldsymbol{x}, t|\boldsymbol{x}_0)|_\Gamma = 0$), and $+\infty$ for a perfectly reactive target with Dirichlet boundary condition ($G_\infty(\boldsymbol{x}, t|\boldsymbol{x}_0)|_\Gamma = 0$). When the confining domain Ω is bounded, the propagator admits a general spectral decomposition

$$G_q(\boldsymbol{x}, t|\boldsymbol{x}_0) = \sum_{k=1}^{\infty} \mathrm{e}^{-Dt\lambda_k^{(q)}} [u_k^{(q)}(\boldsymbol{x})]^*\, u_k^{(q)}(\boldsymbol{x}_0), \tag{7}$$

J. Stat. Mech. (2022) 083205

where asterisk denotes complex conjugate, while $\lambda_k^{(q)}$ and $u_k^{(q)}(\boldsymbol{x})$ are the eigenvalues and eigenfunctions of the (negative) Laplace operator in Ω with mixed Robin–Neumann boundary condition:

$$\Delta u_k^{(q)} + \lambda_k^{(q)} u_k^{(q)} = 0 \quad (\boldsymbol{x} \in \Omega), \tag{8a}$$

$$(\partial_n + q) u_k^{(q)} = 0 \quad (\boldsymbol{x} \in \Gamma), \tag{8b}$$

$$\partial_n u_k^{(q)} = 0 \quad (\boldsymbol{x} \in \partial\Omega_0). \tag{8c}$$

The eigenvalues are positive and indexed in an ascending order,

$$0 < \lambda_1^{(q)} \leqslant \lambda_2^{(q)} \leqslant \cdots \leqslant \lambda_k^{(q)} \cdots \nearrow +\infty,$$

while the eigenfunctions form a complete orthonormal basis in the space $L_2(\Omega)$ of square-integrable functions on Ω (see a review [88] for other properties of Laplacian eigenvalues and eigenfunctions). The superscript q highlights that both $\lambda_k^{(q)}$ and $u_k^{(q)}(\boldsymbol{x})$ depend *implicitly* on the parameter q via the Robin boundary condition (8b).

As the integral of the propagator $G_q(\boldsymbol{x}, t|\boldsymbol{x}_0)$ over the arrival point $\boldsymbol{x}$ yields the survival probability of the particle in the presence of a partially reactive target,

$$S_q(t|\boldsymbol{x}_0) = \int\limits_\Omega \mathrm{d}\boldsymbol{x}\, G_q(\boldsymbol{x}, t|\boldsymbol{x}_0), \tag{9}$$

the latter is directly related to the probability density $\rho(\ell, t|\boldsymbol{x}_0)$ of the boundary local time ℓ_t:

$$S_q(t|\boldsymbol{x}_0) = \int\limits_0^\infty \mathrm{d}\ell\, \mathrm{e}^{-q\ell} \rho(\ell, t|\boldsymbol{x}_0). \tag{10}$$

We recall that $S_q(t|\boldsymbol{x}_0)$ satisfies the (backward) diffusion equation

$$\partial_t S_q(t|\boldsymbol{x}_0) = D\Delta S_q(t|\boldsymbol{x}_0) \quad (\boldsymbol{x}_0 \in \Omega), \tag{11}$$

subject to the initial (terminal) condition $S_q(0|\boldsymbol{x}_0) = 1$ and mixed Robin–Neumann boundary condition:

$$\partial_n S_q(t|\boldsymbol{x}_0) + q S_q(t|\boldsymbol{x}_0) = 0 \quad (\boldsymbol{x}_0 \in \Gamma), \tag{12a}$$

$$\partial_n S_q(t|\boldsymbol{x}_0) = 0 \quad (\boldsymbol{x}_0 \in \partial\Omega_0). \tag{12b}$$

According to equation (7), the survival probability admits a general spectral decomposition

$$S_q(t|\boldsymbol{x}_0) = \sum_{k=1}^\infty \mathrm{e}^{-Dt\lambda_k^{(q)}} [c_k^{(q)}]^* u_k^{(q)}(\boldsymbol{x}_0), \tag{13}$$

J. Stat. Mech. (2022) 083205

where

$$c_k^{(q)} = \int_\Omega \mathrm{d}\boldsymbol{x}\, u_k^{(q)}(\boldsymbol{x}). \tag{14}$$

The inverse Laplace transform of equation (10) with respect to q yields

$$\rho(\ell, t|\boldsymbol{x}_0) = \mathcal{L}_q^{-1}\{S_q(t|\boldsymbol{x}_0)\} = \mathcal{L}_q^{-1}\left\{\sum_{k=1}^{\infty} \mathrm{e}^{-Dt\lambda_k^{(q)}}\, [c_k^{(q)}]^*\, u_k^{(q)}(\boldsymbol{x}_0)\right\}. \tag{15}$$

In the following, we often consider the volume-averaged case when the starting point $\boldsymbol{x}_0$ is not fixed but uniformly distributed inside the confining domain. The corresponding survival probability $S_q(t)$ reads

$$S_q(t) = \frac{1}{|\Omega|}\int_\Omega \mathrm{d}\boldsymbol{x}_0\, S_q(t|\boldsymbol{x}_0) = \sum_{k=1}^{\infty} \frac{|c_k^{(q)}|^2}{|\Omega|}\mathrm{e}^{-Dt\lambda_k^{(q)}}, \tag{16}$$

where $|\Omega|$ denotes the volume of the confining domain Ω. The relation (10) becomes

$$S_q(t) = \int_0^\infty \mathrm{d}q\, \mathrm{e}^{-q\ell}\, \rho(\ell, t), \tag{17}$$

where

$$\rho(\ell, t) = \frac{1}{|\Omega|}\int_\Omega \mathrm{d}\boldsymbol{x}_0\, \rho(\ell, t|\boldsymbol{x}_0) \tag{18}$$

is the probability density function of the boundary local time ℓ_t for a particle started uniformly in the domain Ω.

In the above setting, the bulk was not reactive, and the particle could only react on the target Γ. If restricted diffusion occurs inside a reactive medium, the particle has a finite lifetime due to eventual disintegration, photobleaching or death during its motion [89–91]. In a common situation, the lifetime τ of the particle is a random variable obeying the exponential law, $\mathbb{P}\{\tau > t\} = \mathrm{e}^{-pt}$, with p being the decay rate or, equivalently, $1/p$ being the mean lifetime. In this case, one can investigate the number of encounters with the target during the particle's lifetime: ℓ_τ. The probability density function of this random variable can be easily obtained by averaging $\rho(\ell, t|\boldsymbol{x}_0)$ over all possible times of particle's death:

$$\int_0^\infty \mathrm{d}t\, \underbrace{p\,\mathrm{e}^{-pt}}_{\text{pdf of } \tau}\rho(\ell, t|\boldsymbol{x}_0) = p\tilde{\rho}(\ell, p|\boldsymbol{x}_0), \tag{19}$$

where $\tilde{\rho}(\ell, p|\boldsymbol{x}_0)$ is the Laplace transform of $\rho(\ell, t|\boldsymbol{x}_0)$ with respect to t (here and below, tilde denotes Laplace-transformed quantities with respect to time t). As a consequence,

J. Stat. Mech. (2022) 083205

equation (10) implies

$$\tilde{S}_q(p|\boldsymbol{x}_0) = \int_0^\infty \mathrm{d}\ell\, \mathrm{e}^{-q\ell}\tilde{\rho}(\ell, p|\boldsymbol{x}_0), \tag{20}$$

where $\tilde{S}_q(p|\boldsymbol{x}_0)$ satisfies the modified Helmholtz equation

$$(p - D\Delta)\tilde{S}(p|\boldsymbol{x}_0) = 1 \quad (\boldsymbol{x}_0 \in \Omega), \tag{21}$$

subject to the mixed Robin–Neumann boundary condition:

$$\partial_n \tilde{S}_q(p|\boldsymbol{x}_0) + q\tilde{S}_q(p|\boldsymbol{x}_0) = 0 \quad (\boldsymbol{x}_0 \in \Gamma), \tag{22a}$$

$$\partial_n \tilde{S}_q(p|\boldsymbol{x}_0) = 0 \quad (\boldsymbol{x}_0 \in \partial\Omega_0). \tag{22b}$$

Finally, the Laplace-transformed probability density $\tilde{\rho}(\ell, p|\boldsymbol{x}_0)$ admits another spectral expansion based on the Dirichlet-to-Neumann operator $\mathcal{M}_p$ that associates to a given function $f(\boldsymbol{s})$ on the target Γ another function $g(\boldsymbol{s})$ on that target (see [92–98] for details):

$$\mathcal{M}_p : f(\boldsymbol{s}) \to g(\boldsymbol{s}) = (\partial_n \tilde{u}(\boldsymbol{x}))|_{\boldsymbol{x}=\boldsymbol{s}\in\Gamma}, \tag{23}$$

where $\tilde{u}(\boldsymbol{x})$ satisfies

$$(p - D\Delta)\tilde{u}(\boldsymbol{x}) = 0 \quad (\boldsymbol{x} \in \Omega), \tag{24a}$$

$$\tilde{u}(\boldsymbol{x}) = f(\boldsymbol{x}) \quad (\boldsymbol{x} \in \Gamma), \tag{24b}$$

$$\partial_n \tilde{u}(\boldsymbol{x}) = 0 \quad (\boldsymbol{x} \in \partial\Omega_0). \tag{24c}$$

It is known that $\mathcal{M}_p$ is a pseudo-differential self-adjoint operator, whose positive eigenvalues $\mu_n^{(p)}$ can be ordered as

$$0 \leqslant \mu_0^{(p)} \leqslant \mu_1^{(p)} \leqslant \cdots \leqslant \mu_n^{(p)} \leqslant \cdots \nearrow +\infty,$$

while the associated eigenfunctions $v_n^{(p)}(\boldsymbol{s})$ form a complete orthonormal basis of $L_2(\Gamma)$. The superscript p highlights that both $\mu_n^{(p)}$ and $v_n^{(p)}(\boldsymbol{s})$ depend *implicitly* on the rate p in equation (24a). The following expansion was derived in [43]

$$\tilde{P}(\boldsymbol{x}, \ell, p|\boldsymbol{x}_0) = \tilde{G}_\infty(\boldsymbol{x}, p|\boldsymbol{x}_0)\delta(\ell) + \frac{1}{D}\sum_{n=0}^\infty \mathrm{e}^{-\mu_n^{(p)}\ell}\, [V_n^{(p)}(\boldsymbol{x})]^*\, V_n^{(p)}(\boldsymbol{x}_0), \tag{25}$$

where

$$V_n^{(p)}(\boldsymbol{x}_0) = \int_{\partial\Omega} \mathrm{d}\boldsymbol{s}\, v_n^{(p)}(\boldsymbol{s})\, \tilde{j}_\infty(\boldsymbol{s}, p|\boldsymbol{x}_0) \tag{26}$$

is the projection of the Laplace-transformed probability flux density on the perfectly reactive target, $\tilde{j}_\infty(\boldsymbol{s}, p|\boldsymbol{x}_0) = (-D\partial_n \tilde{G}_\infty(\boldsymbol{x}, p|\boldsymbol{x}_0))_{\boldsymbol{x}=\boldsymbol{s}}$, onto the eigenfunction $v_n^{(p)}(\boldsymbol{s})$.

J. Stat. Mech. (2022) 083205

According to equation (3), one has

$$\tilde{\rho}(\ell, p|\boldsymbol{x}_0) = \tilde{S}_\infty(p|\boldsymbol{x}_0)\delta(\ell) + \sum_{n=0}^{\infty} [C_n^{(p)}]^* \frac{\mu_n^{(p)}}{p} V_n^{(p)}(\boldsymbol{x}_0)\, \mathrm{e}^{-\mu_n^{(p)}\ell}, \tag{27}$$

with

$$C_n^{(p)} = \int\limits_\Gamma \mathrm{d}\boldsymbol{s}\, v_n^{(p)}(\boldsymbol{s}), \tag{28}$$

where we used the identity from [99]:

$$\int\limits_\Omega \mathrm{d}\boldsymbol{x}\, V_n^{(p)}(\boldsymbol{x}) = \frac{D}{p}\mu_n^{(p)} \int\limits_\Gamma \mathrm{d}\boldsymbol{s}\, v_n^{(p)}(\boldsymbol{s}). \tag{29}$$

The inverse Laplace transform of equation (27) with respect to p formally reads

$$\rho(\ell, t|\boldsymbol{x}_0) = S_\infty(t|\boldsymbol{x}_0)\delta(\ell) + \mathcal{L}_p^{-1}\left\{\sum_{n=0}^{\infty} [C_n^{(p)}]^* \frac{\mu_n^{(p)}}{p} V_n^{(p)}(\boldsymbol{x}_0)\, \mathrm{e}^{-\mu_n^{(p)}\ell}\right\}. \tag{30}$$

The first term in equation (30) accounts for the trajectories that have not encountered the target up to time t (with probability $S_\infty(t|\boldsymbol{x}_0)$) so that the associated boundary local time remained zero. In turn, the second term represents the trajectories that have reached the target up to time t and thus have positive ℓ_t. Again using the identity (29), one can also treat the case when the starting point $\boldsymbol{x}_0$ is uniformly distributed in Ω:

$$\rho(\ell, t) = S_\infty(t)\delta(\ell) + \frac{D}{|\Omega|}\mathcal{L}_p^{-1}\left\{\sum_{n=0}^{\infty} |C_n^{(p)}|^2 \frac{[\mu_n^{(p)}]^2}{p^2}\, \mathrm{e}^{-\mu_n^{(p)}\ell}\right\}. \tag{31}$$

In summary, the probability density $\rho(\ell, t|\boldsymbol{x}_0)$ of the boundary local time can be accessed in two complementary ways: either via the inverse Laplace transform (15) with respect to q, or via the inverse Laplace transform (30) with respect to p. These equivalent ways reflect the duality of bulk and surface reaction mechanisms elaborated in [43]. We will employ both ways in the analysis of small targets.

3. Three approaches

This section describes our main theoretical results on the statistics of the boundary local time on a small target. We present three complementary approaches to address this problem. We start in section 3.1 by the MAA, which aims to match two approximate solutions—an inner solution in the vicinity of the target as if the target was located in the free space (without confinement), and an outer solution as if the target was point-like. Our derivation relies on the asymptotic expansion of the Laplace-transformed full propagator $\tilde{P}(\boldsymbol{x}, \ell, p|\boldsymbol{x}_0)$ that was recently obtained by Bressloff [79]. We show the advantages and practical limitations of this general and powerful technique. In section 3.2,

J. Stat. Mech. (2022) 083205

we use a different strategy based on an approximation for the principal eigenvalue of the Laplace operator. In this way, we derive a very simple yet accurate approximation for the probability density of the boundary local time. In section 3.3, we employ yet another approach relying on the SCA. These three approaches provide complementary views onto the statistics of encounters with a small target.

3.1. Matched asymptotic analysis (MAA)

Bressloff developed the MAA for the Laplace-transformed full propagator $\tilde{P}(\boldsymbol{x}, \ell, p|\boldsymbol{x}_0)$ in three dimensions [79]. He considered a configuration of N spherical targets located at points $\boldsymbol{x}_1, \ldots, \boldsymbol{x}_N \in \Omega$ and having small radii $r_1, \ldots, r_N$ (an extension to nonspherical targets was also discussed). The targets were supposed to be located far away from each other:

$$\max_j \{r_j\} \ll \min_{i \neq j} \{|\boldsymbol{x}_i - \boldsymbol{x}_j|\}. \tag{32}$$

In other words, if $R_{\min}$ is the minimal separation distance between targets (the right-hand side), then $r_j/R_{\min} = O(\epsilon)$, where ϵ is a small parameter.

In the leading-order term, Bressloff obtained a very simple relation,

$$\tilde{P}(\boldsymbol{x}, \ell, p|\boldsymbol{x}_0) = \tilde{G}_\infty(\boldsymbol{x}, p|\boldsymbol{x}_0)\delta(\ell) + \tilde{u}_0(\boldsymbol{x}, \ell, p|\boldsymbol{x}_0) + O(\epsilon), \tag{33}$$

where $\tilde{G}_\infty(\boldsymbol{x}, p|\boldsymbol{x}_0)$ is the Laplace transform of the propagator $G_\infty(\boldsymbol{x}, t|\boldsymbol{x}_0)$ defined by equations (5) and (6) with $q = \infty$ (i.e. a perfectly reactive target with Dirichlet boundary condition), and

$$\tilde{u}_0(\boldsymbol{x}, \ell, p|\boldsymbol{x}_0) = 4\pi D \sum_{j=1}^{N} \mathrm{e}^{-\ell/r_j}\, \tilde{g}(\boldsymbol{x}_j, p|\boldsymbol{x}_0)\, \tilde{g}(\boldsymbol{x}, p|\boldsymbol{x}_j), \tag{34}$$

with

$$\tilde{g}(\boldsymbol{x}, p|\boldsymbol{x}_0) = \frac{\mathrm{e}^{-|\boldsymbol{x}-\boldsymbol{x}_0|\sqrt{p/D}}}{4\pi D|\boldsymbol{x} - \boldsymbol{x}_0|} \tag{35}$$

being the fundamental solution of the modified Helmholtz equation in $\mathbb{R}^3$:

$$(p - D\Delta)\tilde{g}(\boldsymbol{x}, p|\boldsymbol{x}_0) = \delta(\boldsymbol{x} - \boldsymbol{x}_0). \tag{36}$$

The next-order term in equation (33) was also determined in [79] but its expression is more sophisticated.

A probabilistic interpretation of equation (33) is instructive. The first term represents the contribution of trajectories that have not encountered any target so that the boundary local time ℓ_t remained zero. In turn, the second term describes the trajectories that reached one of the targets. As the targets are small and well separated, their contributions are independent from each other and thus additive. For the jth target, the factor $\tilde{g}(\boldsymbol{x}_j, p|\boldsymbol{x}_0)$ describes the passage from the starting point $\boldsymbol{x}_0$ to the target location $\boldsymbol{x}_j$, the factor $\mathrm{e}^{-\ell/r_j}$ characterizes the acquired boundary local time, and the factor

J. Stat. Mech. (2022) 083205

$\tilde{g}(\boldsymbol{x}, p|\boldsymbol{x}_j)$ describes the motion from $\boldsymbol{x}_j$ to $\boldsymbol{x}$ (figure 1(a)). We recall that the inverse Laplace transform of this factor,

$$g(\boldsymbol{x}_j, t|\boldsymbol{x}_0) = \frac{1}{(4\pi D t)^{3/2}} \exp\left(-\frac{|\boldsymbol{x}_j - \boldsymbol{x}_0|^2}{4Dt}\right), \tag{37}$$

is the propagator of Brownian motion in the three-dimensional space (without any target). Naturally, the next-order terms account for trajectories that have visited two or many targets (figure 1(b)).

This intuitive picture suggests that the leading-order asymptotic expansion (33) is expected to be most accurate for large p; in fact, thinking of p as the bulk reaction rate, one deals here with a highly reactive medium, in which diffusion between distant points is penalized: the contribution of rare trajectories that visit two or many targets within the particle's lifetime (the $O(\epsilon)$ term in equation (33)) is negligible. Similarly, the possibility of a long excursion started from a single target and returned to it, is also unlikely. In other words, such 'long-range returns' to the target are statistically suppressed. We can therefore anticipate that the following asymptotic results would be accurate at short time. In contrast, the contribution $O(\epsilon)$ is expected to be relevant in the opposite limit $p \to 0$ or, equivalently, at long times. We will come back to these statements in section 4.

If the limitation to small p can be ignored (i.e. if equation (34) can be used for any p), the inverse Laplace transform of equation (33) implies

$$P(\boldsymbol{x}, \ell, t|\boldsymbol{x}_0) = G_\infty(\boldsymbol{x}, t|\boldsymbol{x}_0)\delta(\ell) + u_0(\boldsymbol{x}, \ell, t|\boldsymbol{x}_0) + O(\epsilon), \tag{38}$$

with

$$u_0(\boldsymbol{x}, \ell, t|\boldsymbol{x}_0) = \frac{1}{4\pi D} \sum_{j=1}^{N} \frac{\mathrm{e}^{-\ell/r_j}}{|\boldsymbol{x} - \boldsymbol{x}_j|\,|\boldsymbol{x}_0 - \boldsymbol{x}_j|}\, h(t, |\boldsymbol{x} - \boldsymbol{x}_j| + |\boldsymbol{x}_0 - \boldsymbol{x}_j|), \tag{39}$$

where

$$h(t, x) = \frac{x\,\mathrm{e}^{-x^2/(4Dt)}}{\sqrt{4\pi D t^3}} \tag{40}$$

is the Lévy–Smirnov probability density of the first-passage time to the origin for a one-dimensional Brownian motion started from x. Substituting the asymptotic expansion (38) into equation (3), we get

$$\rho(\ell, t|\boldsymbol{x}_0) = S_\infty(t|\boldsymbol{x}_0)\delta(\ell) + u_0(\ell, t|\boldsymbol{x}_0) + O(\epsilon), \tag{41}$$

where

$$u_0(\ell, t|\boldsymbol{x}_0) = \int_\Omega \mathrm{d}\boldsymbol{x}\, u_0(\boldsymbol{x}, \ell, t|\boldsymbol{x}_0). \tag{42}$$

In order to evaluate this contribution, one can look again at the Laplace-transformed quantity $\tilde{u}_0(\boldsymbol{x}, \ell, p|\boldsymbol{x}_0)$. If p is not too small (say, $\sqrt{p/D}\,\mathrm{diam}\{\Omega\} \gg 1$), the integral of

J. Stat. Mech. (2022) 083205

$\tilde{g}(\boldsymbol{x}, p|\boldsymbol{x}_j)$ over Ω can be accurately approximated by integrating over the whole space $\mathbb{R}^3$:

$$\int\limits_{\Omega} \mathrm{d}\boldsymbol{x}\, \tilde{g}(\boldsymbol{x}, p|\boldsymbol{x}_j) \approx \int\limits_{\mathbb{R}^3} \mathrm{d}\boldsymbol{x}\, \tilde{g}(\boldsymbol{x}, p|\boldsymbol{x}_j) = \frac{1}{p}. \tag{43}$$

As a consequence,

$$\tilde{u}_0(\ell, p|\boldsymbol{x}_0) \approx 4\pi D \sum_{j=1}^{N} \mathrm{e}^{-\ell/r_j}\, \tilde{g}(\boldsymbol{x}_j, p|\boldsymbol{x}_0)\, \frac{1}{p}, \tag{44}$$

from which

$$u_0(\ell, t|\boldsymbol{x}_0) \approx \sum_{j=1}^{N} \frac{\mathrm{e}^{-\ell/r_j}}{|\boldsymbol{x}_j - \boldsymbol{x}_0|} \operatorname{erfc}\left(\frac{|\boldsymbol{x}_j - \boldsymbol{x}_0|}{\sqrt{4Dt}}\right), \tag{45}$$

where $\operatorname{erfc}(z)$ is the complementary error function. This function determines a fully explicit approximation (41) to the probability density $\rho(\ell, t|\boldsymbol{x}_0)$.

Moreover, if the starting point is uniformly distributed over the confining domain Ω, one has

$$\rho(\ell, t) = S_\infty(t)\delta(\ell) + u_0(\ell, t) + O(\epsilon), \tag{46}$$

where

$$u_0(\ell, t) = \frac{1}{|\Omega|} \int\limits_{\Omega} \mathrm{d}\boldsymbol{x}_0\, u_0(\ell, t|\boldsymbol{x}_0). \tag{47}$$

As $u_0(\ell, t|\boldsymbol{x}_0)$ in equation (45) is given as a sum, one can compute $u_0(\ell, t)$ by integrating separately each term. For the jth term, one can introduce local spherical coordinates centered at $\boldsymbol{x}_j$ and ignore the presence of other targets due to the well-separation condition (32). In addition, the earlier assumption of large p is equivalent to considering the short-time limit, in which the upper limit of the integral can be replaced by infinity:

$$\begin{aligned} u_0(\ell, t) &\approx \frac{1}{|\Omega|} \sum_{j=1}^{N} \int\limits_{\Omega} \mathrm{d}\boldsymbol{x}_0 \frac{\mathrm{e}^{-\ell/r_j}}{|\boldsymbol{x}_j - \boldsymbol{x}_0|} \operatorname{erfc}\left(\frac{|\boldsymbol{x}_j - \boldsymbol{x}_0|}{\sqrt{4Dt}}\right) \\ &\approx \frac{1}{|\Omega|} \sum_{j=1}^{N} \mathrm{e}^{-\ell/r_j}\, 4\pi \int\limits_{0}^{\infty} \mathrm{d}r\, r^2 \frac{1}{r} \operatorname{erfc}\left(\frac{r}{\sqrt{4Dt}}\right) = \frac{4\pi D t}{|\Omega|} \sum_{j=1}^{N} \mathrm{e}^{-\ell/r_j}. \end{aligned} \tag{48}$$

For a single target or for multiple *identical* targets (with equal radii $r_j = R$), the leading term of the asymptotic expansions (38), (41), and (46) exhibits the same dependence on ℓ via the factor $\mathrm{e}^{-\ell/R}$. As a consequence, the leading-order expansion can be interpreted as an exponential distribution of the boundary local time ℓ_t, to which a

J. Stat. Mech. (2022) 083205

probability measure atom at $\ell = 0$ is added:

$$\rho(\ell, t|\boldsymbol{x}_0) \approx S_\infty(t|\boldsymbol{x}_0)\delta(\ell) + \mathrm{e}^{-\ell/R}\sum_{j=1}^{N}\frac{1}{|\boldsymbol{x}_j - \boldsymbol{x}_0|}\,\mathrm{erfc}\left(\frac{|\boldsymbol{x}_j - \boldsymbol{x}_0|}{\sqrt{4Dt}}\right) + O(\epsilon), \quad (49)$$

where we used equation (45). Similarly, equation (48) yields for the uniformly distributed starting point:

$$\rho(\ell, t) \approx S_\infty(t)\,\delta(\ell) + \frac{4\pi Dt}{|\Omega|}\mathrm{e}^{-\ell/R}. \quad (50)$$

As the probability densities $\rho(\ell, t|\boldsymbol{x}_0)$ and $\rho(\ell, t)$ must be normalized to 1, the time-dependent prefactors in front of $\delta(\ell)$ and $\mathrm{e}^{-\ell/R}$ should be related as

$$1 = \int_0^\infty \mathrm{d}\ell\,\rho(\ell, t|\boldsymbol{x}_0) = S_\infty(t|\boldsymbol{x}_0) + R\sum_{j=1}^{N}\frac{1}{|\boldsymbol{x}_j - \boldsymbol{x}_0|}\,\mathrm{erfc}\left(\frac{|\boldsymbol{x}_j - \boldsymbol{x}_0|}{\sqrt{4Dt}}\right), \quad (51a)$$

$$1 = \int_0^\infty \mathrm{d}\ell\,\rho(\ell, t) = S_\infty(t) + R\frac{4\pi Dt}{|\Omega|}. \quad (51b)$$

The accuracy of these relations can serve as an indicator of the quality of the exponential-like approximations (49) and (50). As we will discuss in section 4, these relations can be fulfilled for some intermediate range of times but fail in both limits of short and long times. This failure reveals practical limitations of equations (49) and (50). In turn, when the relations (51) are valid, one can replace equations (49) and (50) by their equivalent forms, which automatically respect the normalization:

$$\rho(\ell, t|\boldsymbol{x}_0) \approx S_\infty(t|\boldsymbol{x}_0)\delta(\ell) + (1 - S_\infty(t|\boldsymbol{x}_0))\frac{\mathrm{e}^{-\ell/R}}{R} \quad (52)$$

and

$$\rho(\ell, t) \approx S_\infty(t)\,\delta(\ell) + (1 - S_\infty(t))\frac{\mathrm{e}^{-\ell/R}}{R}, \quad (53)$$

with $S_\infty(t)$ given by equation (16). We will discuss the validity of these exponential-like distributions in section 4.

In summary, one sees that the MAA is a general and powerful technique to access the asymptotic behavior of the full propagator and the related quantities. While the leading-order term of the regular part of the Laplace-transformed full propagator, $\tilde{u}_0(\boldsymbol{x}, \ell, p|\boldsymbol{x}_0)$, admits a simple probabilistic interpretation, its form in time domain is less intuitive. Moreover, getting explicit approximations for the related quantities such as the probability density of the boundary local time, requires further simplifying assumptions that may limit the range of their applicability. Most importantly, the next-order terms accounting for the contribution of trajectories visiting several targets (or performing several 'long-range returns' to a single target) may become relevant at long times. Even though the MAA offers a systematic way to access these terms, their derivation and

J. Stat. Mech. (2022) 083205

dependence on the parameters become much more sophisticated. For this reason, one may search for alternative approaches to get an approximation of the probability density of the boundary local time on a small target.

3.2. Principal eigenvalue approximation (PEA)

When the target is small, the ground eigenfunction of the Laplace operator is nearly constant, $u_1^{(q)}(\boldsymbol{x}) \approx |\Omega|^{-1/2}$, except for a vicinity of the target (see [80] and references therein). As a consequence, the coefficient $c_k^{(q)}$ in equation (14), in which the eigenfunction $u_k^{(q)}$ is projected onto a constant and thus onto $u_1^{(q)}$, can be approximated as $c_k^{(q)} \approx \delta_{k,1}$, where $\delta_{k,1}$ is the Kronecker symbol: $\delta_{k,1} = 1$ for $k = 1$ and 0 otherwise. The ground eigenmode provides therefore the major contribution to the volume-averaged survival probability:

$$S_q(t) \approx \mathrm{e}^{-Dt\lambda_1^{(q)}}. \tag{54}$$

If the small target Γ is located far away from the reflecting boundary $\partial\Omega_0$ of a bounded domain in $\mathbb{R}^d$ with $d \geqslant 3$, the principal eigenvalue can be approximated as [80]:

$$\lambda_1^{(q)} \approx \lambda_1^{(\infty)} \frac{qL}{1+qL}, \qquad \lambda_1^{(\infty)} \approx \frac{C}{|\Omega|}. \tag{55}$$

Here $L = |\Gamma|/C$ was called the trapping length of the target, with $|\Gamma|$ and C being respectively the surface area and the (harmonic) capacity of the target. The eigenvalue $\lambda_1^{(\infty)}$ corresponds to a perfectly reactive target ($q = \infty$) with Dirichlet boundary condition. The validity and high accuracy of the principal eigenvalue approximation (PEA) (55) were confirmed for anisotropic targets in $\mathbb{R}^d$ with several values of $d \geqslant 3$ [80]. Actually, the approximation (55) was getting more and more accurate as d increases. In turn, one may need to include the known first-order correction to the capacity C in three dimensions (see [76, 80] and references therein, as well as equation (79) below). Even though the analysis in [80] was focused on a single target, the derivation remains applicable for multiple, well-separated small targets satisfying the condition (32). In this case, C is the sum of harmonic capacities of all targets, while $|\Gamma|$ is the sum of their surface areas.

Substituting the approximation (55) into equation (54), one can invert the Laplace transform in equation (17) to get

$$\rho(\ell, t) \approx \rho_{\mathrm{PEA}}(\ell, t), \tag{56}$$

where

$$\begin{aligned}
\rho_{\mathrm{PEA}}(\ell, t) &= \mathcal{L}_q^{-1}\left\{\exp\left(-Dt\lambda_1^{(\infty)}\frac{qL}{1+qL}\right)\right\} \\
&= \mathrm{e}^{-Dt\lambda_1^{(\infty)}}\left(\delta(\ell) + \sum_{n=1}^{\infty}\frac{(Dt\lambda_1^{(\infty)})^n}{n!}\mathcal{L}_q^{-1}\{(1+qL)^{-n}\}\right) \\
&= \mathrm{e}^{-Dt\lambda_1^{(\infty)}}\left(\delta(\ell) + \frac{Dt\lambda_1^{(\infty)}}{L}\mathrm{e}^{-\ell/L}\sum_{n=0}^{\infty}\frac{(Dt\lambda_1^{(\infty)}\ell/L)^n}{n!(n+1)!}\right),
\end{aligned} \tag{57}$$

J. Stat. Mech. (2022) 083205

which can also be written as

$$\rho_{\rm PEA}(\ell,t) = {\rm e}^{-t/T}\delta(\ell) + \sqrt{\frac{t/T}{\ell L}}{\rm e}^{-\ell/L-t/T} I_1\Big(2\sqrt{(t/T)(\ell/L)}\Big), \tag{58}$$

with $I_\nu(z)$ being the modified Bessel function of the first kind, and $T = 1/(D\lambda_1^{(\infty)})$. This is one of the main results of the paper. As the factor in front of $\delta(\ell)$ is an approximation of the survival probability $S_\infty(t)$, the first term is again interpreted as the contribution of trajectories that never reached the target up to time t (and thus $\ell_t = 0$). In turn, the second term accounts for the trajectories that arrived onto the target and thus yield positive ℓ_t. Despite its approximate character, this probability density is correctly normalized for any t:

$$\int_0^\infty {\rm d}\ell\, \rho_{\rm PEA}(\ell,t) = 1.$$

When $Dt\lambda_1^{(\infty)}\ell/L \gg 1$, the asymptotic behavior of $I_1(z)$ yields

$$\rho_{\rm PEA}(\ell,t) \approx {\rm e}^{-t/T}\delta(\ell) + \frac{(t/T)^{\frac{1}{4}}}{2\sqrt{\pi}\,(\ell/L)^{\frac{3}{4}}L}\exp\left(-\left(\sqrt{\ell/L} - \sqrt{t/T}\right)^2\right). \tag{59}$$

The moments of ℓ_t can be easily deduced from equation (58):

$$\begin{aligned}\mathbb{E}\{[\ell_t]^k\} &= \int_0^\infty {\rm d}\ell\, \ell^k\, \rho(\ell,t) \approx \sqrt{Dt\lambda_1^{(\infty)}}{\rm e}^{-Dt\lambda_1^{(\infty)}} L^k \int_0^\infty {\rm d}z\, z^{k-1/2}\, {\rm e}^{-z}\, I_1\left(\sqrt{4Dt\lambda_1^{(\infty)}z}\right) \\ &= Dt\lambda_1^{(\infty)}\, L^k\, k!\, {\rm e}^{-Dt\lambda_1^{(\infty)}} M\left(k+1\,;2\,;Dt\lambda_1^{(\infty)}\right),\end{aligned} \tag{60}$$

where $M(a\,;b\,;z)$ is the Kummer's confluent hypergeometric function. Using the Kummer's transformation $M(a\,;b\,;z) = {\rm e}^z M(b-a\,;b\,;-z)$, one checks that for any positive integer k, the right-hand side is a polynomial of $Dt\lambda_1^{(\infty)}$ of order $k-1$. For instance, one gets

$$\mathbb{E}\{\ell_t\} \approx L(Dt\lambda_1^{(\infty)}) \approx Dt|\Gamma|/|\Omega|, \qquad {\rm var}\{\ell_t\} \approx 2L^2(Dt\lambda_1^{(\infty)}), \tag{61}$$

in agreement with general results [42].

The accuracy of this approximation will be discussed in section 4. We stress that the approximation (58) is fully explicit and includes just few geometric parameters: the surface area and the capacity of the target, as well as the volume of the domain. In the case of a spherical target of radius R, one has $|\Gamma| = 4\pi R^2$ and $C = 4\pi R$, i.e. the trapping length is simply $L = R$. However, there is no restriction neither on the shape on the target, nor on the space dimensionality $d \geqslant 3$ (see the discussion of the planar case in section 6). In other words, the approximation is valid for a general confining domain and any small enough target (up to some mathematical restrictions, e.g. on boundary smoothness for a rigorous formulation of the problem).

J. Stat. Mech. (2022) 083205

It is instructive to compare the regular part of the approximation (58) to the exponential-like behavior (53) for a single spherical particle with $L = R$. Despite the common factor $\mathrm{e}^{-\ell/R}$, the dependence on ℓ is more sophisticated in equation (58). In fact, ℓ appears in the argument of the modified Bessel function and is thus coupled to time t, which thus controls the behavior of $I_1(z)$. This can also be seen in the long-time asymptotic relation (59), which exhibits a distinct maximum of the boundary local time ℓ_t around the mean value $Dt\lambda_1^{(\infty)}L$ that grows with time. In contrast, the mean value predicted by equation (53), $R(1 - S_\infty(t))$, approaches a constant R as time t grows. This behavior, which contradicts the general properties of the boundary local time in confined domains, is in turn reminiscent to the case of a spherical target in $\mathbb{R}^3$, as if the reflecting boundary $\partial\Omega_0$ was moved to infinity [42]. Once again, this discrepancy highlights the limitations of the matched asymptotic expansion at long times.

3.3. Self-consistent approximation (SCA)

Even though the PEA provides a simple form of the probability density $\rho(\ell, t)$, it is instructive to discuss yet another approach to this problem. In [82–86], a SCA was developed to calculate the survival probability $S_q(t|\boldsymbol{x}_0)$, in which the mixed boundary condition (22) was replaced by an effective inhomogeneous Neumann boundary condition, with a constant flux on the target. For a small target in a general confining domain, the SCA reads [86]

$$\tilde{S}_q^{\mathrm{app}}(p|\boldsymbol{x}_0) = \frac{1}{p} - \frac{1}{p}\left(\frac{1}{q} + \frac{1}{Q_p}\right)^{-1} F_p(\boldsymbol{x}_0), \tag{62}$$

where

$$\frac{1}{Q_p} = \frac{1}{|\Gamma|}\sum_{n=0}^{\infty} \frac{|C_n^{(p)}|^2}{\mu_n^{(p)}} \tag{63}$$

and

$$F_p(\boldsymbol{x}_0) = \sum_{n=0}^{\infty} \frac{[C_n^{(p)}]^*}{\mu_n^{(p)}} V_n^{(p)}(\boldsymbol{x}_0), \tag{64}$$

with $V_n^{(p)}(\boldsymbol{x}_0)$ and $C_n^{(p)}$ being given by equations (26) and (28). The inversion of the Laplace transform in equation (10) with respect to q yields

$$\tilde{\rho}^{\mathrm{app}}(\ell, p|\boldsymbol{x}_0) = \frac{1 - Q_p F_p(\boldsymbol{x}_0)}{p}\,\delta(\ell) + \frac{Q_p^2\, F_p(\boldsymbol{x}_0)}{p}\,\exp(-Q_p\ell). \tag{65}$$

As previously, the first term represents the contribution of trajectories that do not encounter the target, whereas the second term gives the contribution of trajectories that encountered the target and thus increased the boundary local time. One can easily check that the approximate probability density in equation (65) is correctly normalized:

J. Stat. Mech. (2022) 083205

$$\int_0^\infty \mathrm{d}\ell\, \tilde{\rho}^{\mathrm{app}}(\ell, p|\boldsymbol{x}_0) = \frac{1}{p}. \tag{66}$$

Recalling that $p\,\tilde{\rho}(\ell, p|\boldsymbol{x}_0)$ is the probability density of the boundary local time ℓ_τ acquired until the particle's death, one realizes that equation (65) provides again a simple exponential-like distribution of ℓ_τ, whose parameters are determined by Q_p and $F_p(\boldsymbol{x}_0)$. We stress that the above description has no restriction on the connectivity of the target Γ, i.e. it is applicable to multiple targets as well.

While the probability density (65) has a simple form in the Laplace domain, its parameters Q_p and $F_p(\boldsymbol{x}_0)$ depend on the confining domain and the target in a sophisticated way (via the spectral properties of the Dirichlet-to-Neumann operator). In addition, the inverse Laplace transform with respect to p is still needed to access the probability density function $\rho(\ell, t|\boldsymbol{x}_0)$ of the boundary local time ℓ_t. As a consequence, this approach may look too sophisticated and less informative as compared to the former ones discussed in sections 3.1 and 3.2. At the same time, it brings complementary insights onto the statistics of diffusive encounters, as described below. In addition, the SCA becomes exact in some symmetric domains and can thus be used as a benchmark for validating the accuracy of other approximations (see section 4). Finally, the SCA does not rely on a sufficient separation between the target and the outer boundary (that was required for the principal value approximation in section 3.2), nor on a sufficient separation between targets (that was required for the MAA in section 3.1). In other words, the underlying assumptions are weaker than in two other cases.

When the starting point $\boldsymbol{x}_0$ is uniformly distributed inside the confining domain Ω, the volume average reads:

$$\tilde{\rho}^{\mathrm{app}}(\ell, p) = \frac{1}{|\Omega|}\int_\Omega \mathrm{d}\boldsymbol{x}_0\, \tilde{\rho}^{\mathrm{app}}(\ell, p|\boldsymbol{x}_0) = \frac{1 - Q_p\overline{F_p}}{p}\delta(\ell) + \frac{Q_p^2\overline{F_p}}{p}\mathrm{e}^{-Q_p\ell}, \tag{67}$$

with

$$\overline{F_p} = \frac{1}{|\Omega|}\int_\Omega \mathrm{d}\boldsymbol{x}_0\, F_p(\boldsymbol{x}_0) = \frac{1}{|\Omega|}\sum_{n=0}^\infty \frac{[C_n^{(p)}]^*}{\mu_n^{(p)}}\int_\Omega \mathrm{d}\boldsymbol{x}_0\, V_n^{(p)}(\boldsymbol{x}_0) = \frac{D}{p|\Omega|}\sum_{n=0}^\infty |C_n^{(p)}|^2 = \frac{D|\Gamma|}{p|\Omega|},$$

where we used the identity (29) and employed the completeness of the eigenbasis $\{v_n^{(p)}(\boldsymbol{s})\}$. In appendix A, we provide some complementary insights and probabilistic interpretation of the parameters Q_p and $F_p(\boldsymbol{x}_0)$, and discuss the short-time and long-time asymptotic behaviors of the approximate probability density $\rho^{\mathrm{app}}(\ell, t)$.

In summary, all three approximations are applicable to multiple arbitrarily-shaped small targets, which are well separated from each other and from the outer boundary. The MMA offers a systematic way to access higher-order corrections and thus to control the accuracy; the PEA yields a fully explicit yet accurate expression (58), which is valid even in higher dimensions; finally, the SCA remains rather formal due to its need to access spectral properties of the Dirichlet-to-Neumann operator but yields an exact solution in some simple domains; it is also less restrictive on the arrangement of the targets. While the PEA is probably the most useful for applications, it is based on the

J. Stat. Mech. (2022) 083205

average over a uniformly distributed starting point and therefore does not capture the impact of a fixed starting point, which is accessed in both MMA and SCA. Overall, these three approximations provide complementary tools for studying the distribution of the boundary local time on small targets.

4. Comparison for a spherical target

In order to access the accuracy of the approximations that we derived in section 3, we consider restricted diffusion toward a spherical target of radius R_1 surrounded by an outer concentric reflecting sphere of radius R_2: $\Omega = \{\boldsymbol{x} \in \mathbb{R}^3 : R_1 < |\boldsymbol{x}| < R_2\}$. For this rotation-invariant domain, the eigenmodes of the Laplace operator and of the Dirichlet-to-Neumann operator are well known [63], in particular,

$$\mu_n^{(p)} = -\bigl(\partial_r g_n^{(p)}\bigr)_{|r=R_1}, \tag{68}$$

with

$$g_n^{(p)}(r) = \frac{k_n'(\alpha R_2) i_n(\alpha r) - i_n'(\alpha R_2) k_n(\alpha r)}{k_n'(\alpha R_2) i_n(\alpha R_1) - i_n'(\alpha R_2) k_n(\alpha R_1)}. \tag{69}$$

Here $\alpha = \sqrt{p/D}$, $i_n(z) = \sqrt{\pi/(2z)}\, I_{n+1/2}(z)$ and $k_n(z) = \sqrt{2/(\pi z)}\, K_{n+1/2}(z)$ are the modified spherical Bessel functions of the first and second kind, and the prime denotes the derivative with respect to the argument. The radial functions $g_n^{(p)}(r)$ satisfy the second-order differential equation

$$\left(\partial_r^2 + \frac{2}{r}\partial_r - \frac{n(n+1)}{r^2} - \alpha^2\right) g_n^{(p)}(r) = 0, \tag{70}$$

with $g_n^{(p)}(R_1) = 1$ and $\left(\partial_r g_n^{(p)}\right)_{r=R_2} = 0$.

As the target region covers the whole inner sphere, the survival probability $S_q(t|\boldsymbol{x}_0)$ and the probability density $\rho(\ell, t|\boldsymbol{x}_0)$ of the boundary local time do not depend on the angular spherical coordinates (θ_0, ϕ_0) of the starting point $\boldsymbol{x}_0 = (r_0, \theta_0, \phi_0)$. In addition, the ground eigenfunction $v_0^{(p)}(\boldsymbol{s}) = 1/\sqrt{4\pi R_1^2}$ is constant, and the projection of other eigenfunctions on 1 in equation (28) yields thus

$$C_n^{(p)} = \sqrt{4\pi} R_1\, \delta_{n,0}. \tag{71}$$

Substituting this expression into equation (27), one has

$$\tilde{\rho}(\ell, p|\boldsymbol{x}_0) = \tilde{S}_\infty(p|\boldsymbol{x}_0)\delta(\ell) + \sqrt{4\pi} R_1 \frac{\mu_0^{(p)}}{p} \mathrm{e}^{-\mu_0^{(p)}\ell} V_0^{(p)}(\boldsymbol{x}_0), \tag{72}$$

with

$$\tilde{S}_\infty(p|\boldsymbol{x}_0) = \frac{1 - \tilde{H}_\infty(p|\boldsymbol{x}_0)}{p} = \frac{1 - g_0^{(p)}(r_0)}{p} \tag{73}$$

J. Stat. Mech. (2022) 083205

and

$$V_0^{(p)}(\boldsymbol{x}_0) = \frac{1}{\sqrt{4\pi}R_1}\int\limits_\Gamma \mathrm{d}\boldsymbol{s}\,\tilde{j}_\infty(\boldsymbol{s},p|\boldsymbol{x}_0) = \frac{\tilde{H}_\infty(p|\boldsymbol{x}_0)}{\sqrt{4\pi}R_1} = \frac{g_0^{(p)}(r_0)}{\sqrt{4\pi}R_1}, \tag{74}$$

where $\tilde{H}_\infty(p|\boldsymbol{x}_0)$ is the Laplace-transformed probability density of the first-passage time to a perfectly reactive target. We get thus

$$\tilde{\rho}(\ell,p|\boldsymbol{x}_0) = \frac{1-g_0^{(p)}(r_0)}{p}\delta(\ell) + \frac{g_0^{(p)}(r_0)}{p}\mu_0^{(p)}\,\mathrm{e}^{-\mu_0^{(p)}\ell}. \tag{75}$$

When the starting point $\boldsymbol{x}_0$ is uniformly distributed in Ω, one can use equation (70) to show that

$$\int\limits_{R_1}^{R_2}\mathrm{d}r\,r^2\,g_0^{(p)}(r) = -\frac{R_1^2(\partial_r g_0^{(p)})_{r=R_1}}{p/D} = \frac{DR_1^2\mu_0^{(p)}}{p}, \tag{76}$$

from which

$$\tilde{\rho}(\ell,p) = \left(\frac{1}{p} - \frac{4\pi DR_1^2\mu_0^{(p)}}{p^2|\Omega|}\right)\delta(\ell) + \frac{4\pi DR_1^2[\mu_0^{(p)}]^2}{p^2|\Omega|}\mathrm{e}^{-\mu_0^{(p)}\ell}. \tag{77}$$

Equations (75) and (77) provide the exact form of the probability density in the Laplace domain. In the following, we focus on equation (77) and perform its inverse Laplace transform with respect to p numerically to get the probability density $\rho(\ell,t)$. Despite this numerical step, this solution will be referred to as an exact solution, to which other approximations will be compared.

The substitution of equation (71) into equations (63) and (64) yields

$$Q_p = \mu_0^{(p)}, \qquad F_p(\boldsymbol{x}_0) = \frac{g_0^{(p)}(r_0)}{\mu_0^{(p)}}, \tag{78}$$

so that the approximate probability density $\tilde{\rho}^{\mathrm{app}}(\ell,p|\boldsymbol{x}_0)$ from equation (65) turns out to be identical with the exact one given by equation (75). In other words, the SCA is *exact* for the considered case. We emphasize that this is a consequence of the rotation symmetry; in general, the SCA does not coincide with the exact solution.

A comparison with the PEA (58) is straightforward. In fact, the capacity C of a spherical target is equal to $4\pi R_1$. As discussed in [80], a more accurate approximation involves the 'corrected' capacity, which for a spherical target reads as

$$C' = C(1 - CR(\boldsymbol{x}_\Gamma,\boldsymbol{x}_\Gamma)), \tag{79}$$

where $R(\boldsymbol{x}_T,\boldsymbol{x}_T)$ is the regular part of the Neumann's Green function, evaluated at the location $\boldsymbol{x}_T$ of the target inside the confining spherical domain of radius R_2 [76]:

$$(4\pi R_2)\,R(\boldsymbol{x},\boldsymbol{x}) = \frac{1}{1-\frac{|\boldsymbol{x}|^2}{R_2^2}} - \ln\left(1-\frac{|\boldsymbol{x}|^2}{R_2^2}\right) + \frac{|\boldsymbol{x}|^2}{R_2^2} - \frac{14}{5}. \tag{80}$$

J. Stat. Mech. (2022) 083205

In our case, the target is located at the origin, $\boldsymbol{x}_T = \mathbf{0}$, so that

$$C' = 4\pi R_1 \left(1 + \frac{9R_1}{5R_2}\right), \tag{81}$$

and thus

$$\lambda_1^{(\infty)} \approx \frac{C'}{|\Omega|} \approx \frac{3R_1(1 + (9R_1)/(5R_2))}{R_2^3}, \tag{82}$$

$$L = \frac{|\Gamma|}{C'} = \frac{R_1}{1 + (9R_1)/(5R_2)}, \tag{83}$$

where we neglected the small term R_1^3 as compared to R_2^3 in the volume $|\Omega|$.

Figure 2 compares several approximations of the probability density $\rho(\ell, t)$ to the exact solution obtained via a numerical inverse Laplace transform of the exact relation (75). As the singular term $S_\infty(t)\delta(\ell)$ is the same for all considered approximations, we present only the regular part of $\rho(\ell, t)$, which allows one to appreciate the quality of these approximations. Setting $R_2 = 1$ and $D = 1$ fixes the units of length and time. In the considered example, we choose a relatively small target with $R_1/R_2 = 0.1$, for which the volume-averaged mean first-passage time is $T \simeq 1/(D\lambda_1^{(\infty)}) \approx R_2^3/(3R_1D) \approx 3$. At short times t (as compared to T), the survival probability $S_\infty(t)$ is close to 1, i.e. most trajectories have not yet encountered the target, and $\ell_t = 0$. In this regime, the singular term $S_\infty(t)\delta(\ell)$ provides the dominant contribution to $\rho(\ell, t)$. In turn, the regular part accounts for contributions from rare trajectories that started from the vicinity of the target and have encountered it. The panels (a) and (b) of figure 2 illustrate the dependence of the regular part on ℓ in this regime. One sees that three approximations (50), (53) and (58) are in good agreement with the exact solution, especially in the case $t = 1$. Some deviations on the panel (a) for $t = 0.1$ will be discussed below.

In the opposite long-time regime $t \gg T$, $S_\infty(t)$ is close to 0, and the dominant contribution comes from the regular part of $\rho(\ell, t)$ that is shown on panels (c) and (d) of figure 2. While the PEA (58) remains to be in excellent agreement with the exact solution, exponential-like approximations (50) and (53) based on the MAA, fail at long times. As discussed in section 3.1, the leading-order term does not account for multiple 'long-range returns' of the particle to the target, which substantially modify the statistics of the boundary local time. Even though the MAA allows one to obtain next-order terms, their derivation and resulting expressions rapidly become too cumbersome for a practical implementation. In contrast, the PEA (58), which is remarkably simple and general, fully describes the distribution of ℓ_t. Its excellent quality is rationalized in appendix A, in which equation (58) was re-derived from the long-time asymptotic behavior of the SCA. We recall that the SCA (65) itself is identical to the exact solution for this geometric setting and thus is not discussed here. Figure 3 illustrates the long-time asymptotic relation (59), which follows from the PEA. Expectedly, it is accurate at long times $t = 10$ and $t = 100$ but exhibits deviations at shorter time $t = 1$.

It is instructive to return to the panel (a) and inspect eventual deviations at short times. Such deviations for the PEA are briefly discussed at the end of appendix A. Let

J. Stat. Mech. (2022) 083205

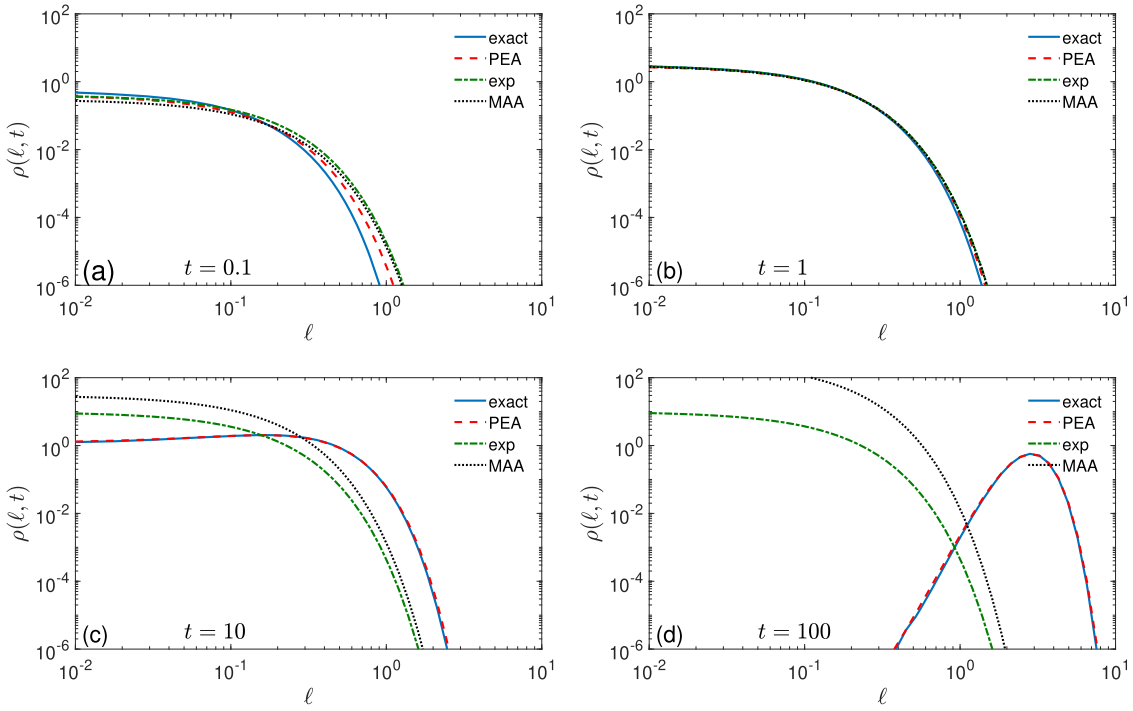

Figure 2. The regular part of the probability density $\rho(\ell, t)$ of the boundary local time ℓ_t on a spherical target of radius $R_1 = 0.1$ surrounded by a concentric reflecting sphere of radius $R_2 = 1$, with $D = 1$, the uniform starting point, and several values of time: $t = 0.1$ (a), $t = 1$ (b), $t = 10$ (c), and $t = 100$ (d). Solid line presents the benchmark solution obtained via a numerical inverse Laplace transform of the exact relation (77) by the Talbot algorithm; dashed line shows the PEA in equation (58); dash-dotted line shows an exponential approximation (53), in which $S_\infty(t)$ was computed via its spectral expansion; dotted line indicates the short-time behavior (50) predicted by the MAA.

us thus focus on deviations of the exponential-like distribution (50) predicted by the MAA. As this relation was obtained by using the short-time approximation, one might expect that equation (50) would be more and more accurate as t goes to 0. This is not the case. In fact, the normalization of the probability density $\rho(\ell, t)$ yields the condition (51b), which reads as

$$\frac{1 - S_\infty(t)}{R} \approx \frac{4\pi D t}{|\Omega|}. \tag{84}$$

This relation can be considered as a necessary condition for the consistence of the approximation (50). Clearly, this relation fails at long times, at which $S_\infty(t)$ vanishes. Is it correct at short times? The answer is negative. In fact, the short-time asymptotic behavior of the survival probability follows from the heat content asymptotics [100–103] and reads [104]

$$S_\infty(t) \approx 1 - \frac{2|\Gamma|}{\sqrt{\pi}|\Omega|}\sqrt{Dt} + O(t). \tag{85}$$

J. Stat. Mech. (2022) 083205

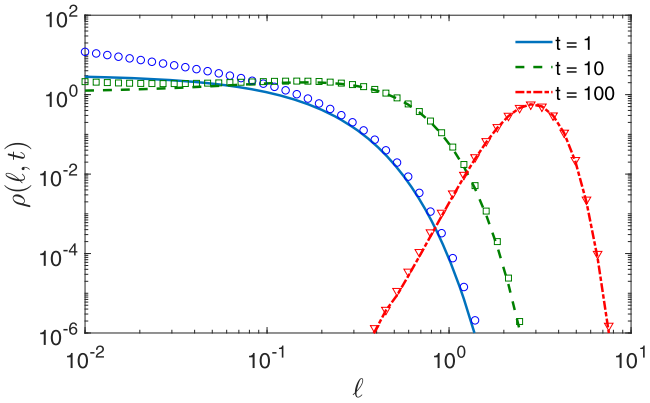

Figure 3. The regular part of the probability density $\rho(\ell, t)$ of the boundary local time ℓ_t on an inner sphere of radius $R_1 = 0.1$ surrounded by an outer reflecting sphere of radius $R_2 = 1$, with $D = 1$ and several values of t. Lines present a numerically inverted Laplace transform of the exact relation (77) by the Talbot algorithm, whereas symbols show the large-ℓ approximation (59).

In other words, since the left-hand side of equation (84) scales as $t^{1/2}$, while the right-hand side does as t, this relation cannot hold at short times. Fortunately, there is an intermediate range of time scales at which equation (84) holds. In fact, if the target is small enough, the survival probability can be approximated via equation (54), which at moderately short times admits the Taylor expansion:

$$S_\infty(t) \approx 1 - Dt\lambda_1^{(\infty)} + O(t^2). \tag{86}$$

and thus equation (51b) is equivalent to $\lambda_1^{(\infty)} \approx 4\pi R_1/|\Omega|$. As the numerator of the right-hand side is precisely the capacity of a spherical target of radius R_1, we retrieve the approximation given in equation (55). In other words, even though the condition (84) fails in both limits $t \to 0$ and $t \to \infty$, it is fulfilled at intermediate times if the target is small enough. We conclude that the exponential-like distribution (50) is valid whenever the PEA (58) is. The latter is therefore much more general.

To complete this discussion, we provide some qualitative arguments why the predictions of the MAA fail at very short times. In this regime, the only nontrivial contribution comes from a very thin layer near the target. At the same time, the main idea of the MAA consists in matching inner and outer solutions of the problem. For the other solution, the target is treated as point-like (for instance, equation (34) involves the fundamental solution $\tilde{g}(\boldsymbol{x}, p|\boldsymbol{x}_0)$ of the modified Helmholtz equation, which deals with a point-like source), so that its geometric structure is not accessible at short times. In other words, the MAA focuses on the limit, in which the target size is the smallest parameter of the problem; in particular, R_1 should be much smaller than a diffusion length $\sqrt{Dt}$. This condition yields a natural restriction of considering not too short times, namely, $t \gg R_1^2/D$. This qualitative argument explains why the agreement on panel (a) for $t = 0.1$ is still acceptable, despite some minor deviations. In turn, deviations are more significant for even small t (not shown).

J. Stat. Mech. (2022) 083205

5. Distribution of first-crossing times

As the PEA turns out to be the most convenient, one can apply it to investigate other properties of the boundary local time and related quantities. Integrating the series expansion (57) of $\rho_{\rm PEA}(\ell,t)$ term by term, we also get an approximation

$$\begin{aligned}\mathbb{P}\{\ell_t>\ell\} &= \int_\ell^\infty {\rm d}\ell'\,\rho(\ell',t) \approx \int_\ell^\infty {\rm d}\ell'\,\rho_{\rm PEA}(\ell',t)\\ &= {\rm e}^{-Dt\lambda_1^{(\infty)}-\ell/L}\sum_{n=0}^\infty \frac{(Dt\lambda_1^{(\infty)})^{n+1}}{(n+1)!}\sum_{k=0}^n \frac{(\ell/L)^k}{k!}\end{aligned} \tag{87}$$

that determines the cumulative distribution function of ℓ_t. Alternatively, one can integrate directly the final expression (58), which yields after changing the integration variable

$$\mathbb{P}\{\ell_t>\ell\} \approx \sqrt{4Dt\lambda_1^{(\infty)}}\,{\rm e}^{-Dt\lambda_1^{(\infty)}}\int_{\sqrt{\ell/L}}^\infty {\rm d}z\,{\rm e}^{-z^2}\,I_1\Big(z\sqrt{4Dt\lambda_1^{(\infty)}}\Big). \tag{88}$$

The function $\mathbb{P}\{\ell_t>\ell\}$ determines also the distribution of the first-crossing time $\mathcal{T}_\ell = \inf\{t>0:\ell_t>\ell\}$ of a given threshold ℓ by the boundary local time ℓ_t, which plays an important role in diffusion-controlled reactions [43]. In fact, since ℓ_t is a non-decreasing process, one has $\mathbb{P}\{\ell_t>\ell\} = \mathbb{P}\{\mathcal{T}_\ell<t\}$, from which the probability density of $\mathcal{T}_\ell$ follows as

$$U(\ell,t) = \partial_t\mathbb{P}\{\mathcal{T}_\ell<t\} = \partial_t\mathbb{P}\{\ell_t>\ell\}. \tag{89}$$

Evaluating the time derivative of equation (87) term by term, we get the following approximation:

$$U_{\rm PEA}(\ell,t) = \frac{1}{T}\,{\rm e}^{-\ell/L-t/T}\,I_0\Big(2\sqrt{(t/T)(\ell/L)}\Big). \tag{90}$$

This is one of the main results of the paper. Despite its approximate character, this probability density is correctly normalized. For large ℓ or t, the asymptotic behavior of $I_0(z)$ yields

$$U_{\rm PEA}(\ell,t) \approx \frac{\exp\Big(-\Big(\sqrt{\ell/L}-\sqrt{t/T}\Big)^2\Big)}{2\sqrt{\pi}(T)^{\frac{3}{4}}\,t^{\frac{1}{4}}\,(\ell/L)^{\frac{1}{4}}}. \tag{91}$$

The moments of $\mathcal{T}_\ell$ can be easily accessed:

J. Stat. Mech. (2022) 083205

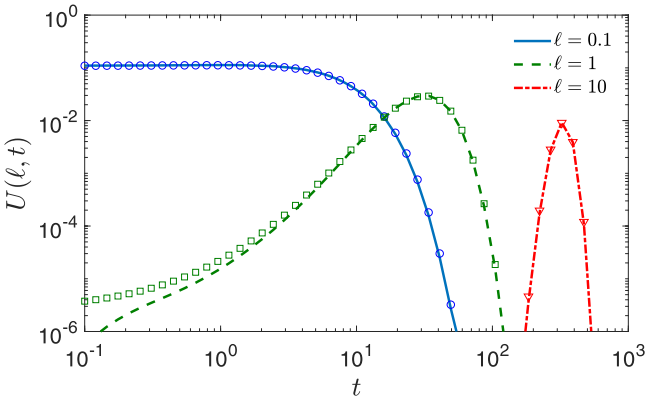

Figure 4. The probability density $U(\ell, t)$ of the first-crossing time $\mathcal{T}_\ell$ of the boundary local time ℓ_t on an inner sphere of radius $R_1 = 0.1$ surrounded by an outer reflecting sphere of radius $R_2 = 1$, with $D = 1$ and several values of the threshold ℓ. Lines present a numerically inverted Laplace transform of the exact relation (94) by the Talbot algorithm, whereas symbols show the PEA (90).

$$\mathbb{E}\{[\mathcal{T}_\ell]^k\} = \int_0^\infty \mathrm{d}t\, t^k\, U(\ell,t) \approx \frac{\mathrm{e}^{-\ell/L}}{(D\lambda_1^{(\infty)})^k} \int_0^\infty \mathrm{d}z\, z^k\, \mathrm{e}^{-z}\, I_0\Big(2\sqrt{z\ell/L}\Big)$$
$$= T^k k!\, \mathrm{e}^{-\ell/L} M(k+1\,;1\,;\ell/L). \tag{92}$$

For instance, one gets

$$\mathbb{E}\{\mathcal{T}_\ell\} \approx (1+\ell/L)\, T, \qquad \mathrm{var}\{\mathcal{T}_\ell\} \approx (1+2\ell/L)\, T^2. \tag{93}$$

Note that the probability density $U(\ell, t)$ can formally be accessed from the general exact representation (31), which yields for the spherical case:

$$U(\ell,t) = \mathcal{L}_p^{-1}\left\{ \frac{4\pi D R_1^2 \mu_0^{(p)}}{p|\Omega|} \mathrm{e}^{-\mu_0^{(p)}\ell} \right\}. \tag{94}$$

A numerical inversion of this Laplace transform can be used as a benchmark for validating our approximation. Figure 4 illustrates an excellent accuracy of the approximation (90) for several values of the threshold ℓ when t is not too small. In turn, the approximation fails in the small-time limit. In fact, equation (90) suggests that $U(\ell, t) \to D\lambda_1^{(\infty)}\, \mathrm{e}^{-\ell/L}$ as $t \to 0$, whereas the exact solution (94) implies a rapid decay of $U(\ell, t)$. This can be seen from the large-p asymptotic analysis of equation (68) that yields $\mu_0^{(p)} \approx \sqrt{p/D} + 1/R_1$ for the considered spherical case, from which the inverse Laplace transform in equation (94) implies

$$U(\ell,t) \approx \frac{|\Gamma|D}{|\Omega|} \mathrm{e}^{-\ell/R_1} \left(\frac{e^{-\ell^2/(4Dt)}}{\sqrt{\pi D t}} + \frac{1}{R_1} \mathrm{erfc}\left(\frac{\ell}{\sqrt{4Dt}} \right) \right) \quad (t \to 0). \tag{95}$$

J. Stat. Mech. (2022) 083205

The short-time deviation of the approximation (90) is clearly seen in figure 4 for the case $\ell = 1$. Despite this limitation at short times, the simple explicit form of equation (90) captures the behavior of the probability density $U(\ell, t)$ remarkably well.

6. Conclusion

We studied the distribution of the boundary local time ℓ_t, i.e. a rescaled number of encounters between a diffusing particle and a target. This distribution can formally be obtained either by the inverse Laplace transform of the survival probability with respect to the reactivity parameter q, or as an expansion over the eigenbasis of the Dirichlet-to-Neumann operator. In both cases, the underlying quantities depend on the shapes of the confining domain and of the target in a sophisticated, generally unknown way. To access this distribution in the case of a *small* target, we employed three approximations: the MAA, the PEA, and the SCA. The leading order of the MAA yielded an exponential-like distribution (53), with an atom at $\ell = 0$ corresponding to the trajectories that never encountered the target. This approximation was shown to be accurate only at intermediate times but failing in both short- and long-time limits. Such an approximation can be potentially improved by considering higher-order corrections in the MAA which, however, are much more cumbersome. In turn, the PEA provided a simple, fully explicit and remarkably accurate approximation (58). This approximation involves only few geometric characteristics such as the surface area and the harmonic capacity of the target, as well as the volume of the confining domain. In particular, it reveals how the boundary local time ℓ is coupled to physical time t. This is a rare example of an explicitly known distribution of the boundary local time (for two other basic examples, the half-line and the exterior of a sphere, see [65]). The third approach was based on the SCA, which yielded a compact form of the probability density of the boundary local time in the Laplace domain. The need for the Laplace inversion to come back in time domain makes this approximation less appealing in comparison to the PAE. Nevertheless, the SCA-based relations (65) and (67) allowed us to study the asymptotic behaviors; in particular, we managed to retrieve the PEA (58) as the long-time asymptotic limit of the SCA. The accuracy of different approximations was checked in a typical geometric setting of a spherical target surrounded by a reflecting sphere.

It is worth noting that the inversion of the Laplace transform is actually not needed for some applications. For instance, when a particle diffuses in a reactive medium or has an internal destructive mechanism (aging, radioactive decay, photobleaching, nuclear spin relaxation, etc), its lifetime τ is random and usually described by an exponential law with the decay rate p [89–91]. In this case, the above approximations give a direct access to the probability density $p\,\tilde{\rho}(\ell, p|\boldsymbol{x}_0)$ of the boundary local time ℓ_τ, which is stopped at a random time τ. Here, ℓ_τ characterizes the number of encounters with the target until the particle's death. For instance, equation (65) shows that $p\,\tilde{\rho}(\ell, p|\boldsymbol{x}_0)$ admits a simple exponential-like form, with an atom at 0. Moreover, the small-p expansion of the Laplace-transformed probability density $\tilde{\rho}(\ell, p|\boldsymbol{x}_0)$ determines the moments of the boundary local time ℓ_t. Other quantities such as splitting probabilities and conditional first-passage time moments can also be accessed [79].

J. Stat. Mech. (2022) 083205

This paper was mainly focused on three-dimensional confining domains. In particular, this choice allowed us to compare three approximations given that the MAA was done by Bressloff only in three dimensions [79]. Its extension to other space dimensions is in principle feasible but requires additional work. In turn, the SCA was formulated in terms of the eigenbasis of the Dirichlet-to-Neumann operator and is thus valid for any dimension. Finally, the PEA (55) is applicable for any $d \geqslant 3$; moreover, it is getting more accurate as d increases [80]. We therefore expect that our approximation (58) for the probability density $\rho(\ell, t)$ would also be accurate in higher dimensions. In turn, the two-dimensional case was excluded from the analysis in [80]. In fact, the harmonic capacity does not exist in two dimensions, whereas solutions of the Laplace equation are much more sensitive to a distant outer boundary. At the same time, one can still consider equation (55) as an interpolation between two limits of perfectly reactive ($q \to \infty$) and weakly reactive ($q \to 0$) targets. Setting $C = \lambda_1^{(\infty)}|\Omega|$ and thus $L = |\Gamma|/(\lambda_1^{(\infty)}|\Omega|)$, one sees that equation (55) interpolates between the limit $\lambda_1^{(\infty)}$ as $q \to \infty$ and the expected behavior $\lambda_1^{(q)} \approx q|\Gamma|/|\Omega|$ as $q \to 0$. Admitting this interpolation, one can keep the derivation in section 3.2 and thus retrieve again the approximation (58) in two dimensions. Moreover, the eigenvalue $\lambda_1^{(\infty)}$ can also be related to the geometric properties of a small target [68–70]. Numerical validation of this conjectural extension to the two-dimensional case presents an interesting perspective.

While we were mainly interested in the distribution of the boundary local time ℓ_t, the approximation (58) allowed us to access the tightly related probability density $U(\ell, t)$ of the first-crossing time $\mathcal{T}_\ell$ of a given threshold ℓ by ℓ_t. Our approximation (90) is a rare example when this probability density admits a fully explicit form. As discussed in [43], this distribution is directly related to the distribution of first-reaction times on a partially reactive target. Moreover, one can go beyond the conventional constant reactivity framework (described by the Robin boundary condition) and deal with other surface reaction mechanisms such as encounter-dependent reactivity. A simple explicit form of the probability density $U(\ell, t)$ allows one to investigate a broad class of first-passage times related to various surface reaction mechanisms. The explicit form of $U(\ell, t)$ can also be employed to study in more detail the resource depletion problem by a population of diffusing particles [105].

Appendix A. Analysis of the self-consistent approximation

In this appendix, we discuss the probabilistic interpretation of the parameters Q_p and $F_p(\boldsymbol{x}_0)$ that determine the SCA, as well as its short-time and long-time asymptotic behaviors.

A.1. Complementary insights

Let us gain complementary insights onto the parameters Q_p and $F_p(\boldsymbol{x}_0)$. Since the kernel of the Dirichlet-to-Neumann operator $\mathcal{M}_p$ is $D\tilde{G}_0(\boldsymbol{s}, p|\boldsymbol{s}_0)$ (see [43]), the expression (63) can also be written as

J. Stat. Mech. (2022) 083205

$$\frac{1}{Q_p} = \frac{1}{|\Gamma|}\int\limits_\Gamma \mathrm{d}\boldsymbol{s}_0 \int\limits_\Gamma \mathrm{d}\boldsymbol{s}\, D\tilde{G}_0(\boldsymbol{s}, p|\boldsymbol{s}_0). \tag{A.1}$$

In order to interpret this expression, we recall that the mean residence time in a subset $A \subset \Omega$ is

$$R_A(t|\boldsymbol{x}_0) = \mathbb{E}_{\boldsymbol{x}_0}\left\{\int\limits_0^t \mathrm{d}t' \mathbb{I}_A(\mathbf{X}_{t'})\right\} = \int\limits_0^t \mathrm{d}t' \int\limits_A \mathrm{d}\boldsymbol{x}\, \mathbb{E}_{\boldsymbol{x}_0}\{\delta(\boldsymbol{x} - \mathbf{X}_{t'})\}$$
$$= \int\limits_0^t \mathrm{d}t' \int\limits_A \mathrm{d}\boldsymbol{x}\, G_0(\boldsymbol{x}, t'|\boldsymbol{x}_0).$$

If A is a thin layer near the target, $A = \Gamma_a$, then we get the mean boundary local time on Γ:

$$\mathbb{E}_{\boldsymbol{x}_0}\{\ell_t\} = \lim_{a\to 0} \frac{D}{a} R_{\Gamma_a}(t|\boldsymbol{x}_0) = \int\limits_0^t \mathrm{d}t' \int\limits_\Gamma \mathrm{d}\boldsymbol{x}\, DG_0(\boldsymbol{x}, t'|\boldsymbol{x}_0), \tag{A.2}$$

where we used that $G_0(\boldsymbol{x}, t'|\boldsymbol{x}_0)$ behaves smoothly in a vicinity of a smooth boundary. If the particle has a finite lifetime, one has to average over t with an exponential probability density:

$$\mathbb{E}_{\boldsymbol{x}_0}\{\ell_\tau\} = \int\limits_0^\infty \mathrm{d}t \underbrace{p\,\mathrm{e}^{-pt}}_{\text{pdf of } \tau} \mathbb{E}_{\boldsymbol{x}_0}\{\ell_t\} = \int\limits_\Gamma \mathrm{d}\boldsymbol{x}\, D\tilde{G}_0(\boldsymbol{x}, p|\boldsymbol{x}_0). \tag{A.3}$$

Note that the inverse Laplace transform of $\mathbb{E}_{\boldsymbol{x}_0}\{\ell_\tau\}/p$ yields the mean $\mathbb{E}_{\boldsymbol{x}_0}\{\ell_t\}$. We conclude that $1/Q_p$ in equation (A.1) is the mean boundary local time ℓ_τ on Γ, averaged over the starting point $\boldsymbol{x}_0$ uniformly distributed on Γ.

For a fixed starting point, one can use equation (65) to approximate the moments of the boundary local time ℓ_τ, in particular, the mean is

$$\mathbb{E}_{\boldsymbol{x}_0}\{\ell_\tau\} \approx \int\limits_0^\infty \mathrm{d}\ell\, \ell\, p\, \tilde{\rho}^{\mathrm{app}}(\ell, p|\boldsymbol{x}_0) = F_p(\boldsymbol{x}_0). \tag{A.4}$$

Its average over $\boldsymbol{x}_0 \in \Gamma$ reads

$$\frac{1}{|\Gamma|}\int\limits_\Gamma \mathrm{d}\boldsymbol{x}_0\, F_p(\boldsymbol{x}_0) = \frac{1}{Q_p}, \tag{A.5}$$

so that

$$\frac{1}{|\Gamma|}\int\limits_\Gamma \mathrm{d}\boldsymbol{x}_0\, p\, \tilde{\rho}^{\mathrm{app}}(\ell, p|\boldsymbol{x}_0) = Q_p\, \exp(-Q_p\ell). \tag{A.6}$$

J. Stat. Mech. (2022) 083205

In summary, if the starting point is uniformly distributed over the target Γ, the distribution of the boundary local time ℓ_τ is close to be exponential, with the mean value $1/Q_p$.

A.2. Long-time behavior

It is instructive to look at the long-time behavior of the approximate probability density $\rho^{\rm app}(\ell, t)$ that follows from the small-p asymptotic analysis of equation (67).

In the limit $p \to 0$, one can apply a standard perturbation theory discussed in [42]. Adapting this approach to our setting with a target Γ surrounded by a reflecting boundary $\partial\Omega_0$, we get

$$\mu_0^{(p)} \approx \frac{|\Omega|}{D|\Gamma|} p + \frac{bp^2}{2} + O(p^3), \tag{A.7}$$

where the parameter b can be represented as

$$b \equiv \lim_{p\to 0} \frac{\mathrm{d}^2 \mu_0^{(p)}}{\mathrm{d}p^2} = -\frac{2|\Omega|^2}{D|\Gamma|^3} \int\limits_\Gamma \mathrm{d}\boldsymbol{s}_1 \int\limits_\Gamma \mathrm{d}\boldsymbol{s}_2\, \mathcal{G}(\boldsymbol{s}_1, \boldsymbol{s}_2),$$

with

$$\mathcal{G}(\boldsymbol{s}_1, \boldsymbol{s}_2) = \lim_{p\to 0} \left(\tilde{G}_0(\boldsymbol{s}, p|\boldsymbol{s}_0) - \frac{1}{p|\Omega|} \right) \tag{A.8}$$

being the Neumann pseudo-Green's function. In turn, the corresponding eigenfunction behaves as $v_0^{(p)}(\boldsymbol{s}) \approx |\Gamma|^{-1/2} + p v_0^1(\boldsymbol{s}) + O(p^2)$ as $p \to 0$. As a consequence, $C_n^{(p)} \approx O(p)$ for $n > 0$ due to the orthogonality of eigenfunctions $v_n^{(p)}$ to $v_0^{(p)}$ (and thus to a constant), in the leading order in p. In turn, the normalization of the eigenfunction $v_0^{(p)}$ implies

$$1 = \|v_0^{(p)}\|^2_{L_2(\Gamma)} = \underbrace{\|v_0^{(0)}\|^2_{L_2(\Gamma)}}_{=1} + 2p\Big(v_0^{(0)} \cdot v_0^1\Big)_{L_2(\Gamma)} + O(p^2),$$

and thus $(v_0^{(0)} \cdot v_0^1)_{L_2(\Gamma)} = 0$, i.e. the integral of the first-order correction $v_0^1(\boldsymbol{s})$ vanishes. As a consequence, $C_0^{(p)} \approx |\Gamma|^{1/2} + O(p^2)$ (i.e. there is no $O(p)$ term). Substituting these relations into equation (63), we get

$$Q_p^{-1} \approx \frac{D|\Gamma|}{p|\Omega|} + L + O(p), \qquad \text{with } L = -\frac{b}{2}(D|\Gamma|/|\Omega|)^2, \tag{A.9}$$

which can also be written as

$$Q_p \approx \frac{|\Omega|}{D|\Gamma|} \frac{p}{1 + p\delta}, \qquad \text{with } \delta = L\frac{|\Omega|}{D|\Gamma|}, \tag{A.10}$$

where we neglected the next-order terms. Substituting this expression into equation (67), we get

J. Stat. Mech. (2022) 083205

$$\tilde{\rho}^{\rm app}(\ell,p) \approx \frac{\delta}{1+p\delta}\delta(\ell) + \frac{\delta/L}{(1+p\delta)^2}{\rm e}^{-(\ell/L)p\delta/(1+p\delta)}. \tag{A.11}$$

The inverse Laplace transform with respect to p reads

$$\begin{aligned}\rho^{\rm app}(\ell,t) &\approx {\rm e}^{-t/\delta}\delta(\ell) + \frac{\delta}{L}{\rm e}^{-\ell/L}\mathcal{L}_p^{-1}\left\{\frac{{\rm e}^{(\ell/L)/(1+p\delta)}}{(1+p\delta)^2}\right\} \\ &= {\rm e}^{-t/\delta}\delta(\ell) + \frac{\delta}{L}{\rm e}^{-\ell/L}\sum_{n=0}^{\infty}\frac{(\ell/L)^n}{n!}\mathcal{L}_p^{-1}\left\{\frac{1}{(1+p\delta)^{n+2}}\right\} \\ &= {\rm e}^{-t/\delta}\delta(\ell) + {\rm e}^{-\ell/L}\,{\rm e}^{-t/\delta}\frac{\sqrt{t/\delta}}{\sqrt{\ell L}}\sum_{n=0}^{\infty}\frac{((\ell/L)t/\delta)^{n+\frac{1}{2}}}{n!(n+1)!} \\ &= {\rm e}^{-t/\delta}\delta(\ell) + {\rm e}^{-\ell/L}\,{\rm e}^{-t/\delta}\frac{\sqrt{t/\delta}}{\sqrt{\ell L}}I_1\Big(2\sqrt{(\ell/L)t/\delta}\Big).\end{aligned} \tag{A.12}$$

Remarkably, the long-time asymptotic relation (A.12) coincides with the PEA (58) from section 3.2, with a different notation $L = |\Gamma|/C$, where C is the capacity of the target. Using this relation, we obtain an interesting representation for the second derivative of $\mu_0^{(p)}$:

$$b \approx -\frac{2|\Omega|^2}{C|\Gamma|D^2}. \tag{A.13}$$

Moreover, substituting this expression into the definition of δ, we get $\delta = |\Omega|/(DC) = 1/(D\lambda_1^{(\infty)})$, i.e. we retrieve an approximation $\lambda_1^{(\infty)} = C/|\Omega|$ for the principal eigenvalue for the perfect target. In this way, two approaches result in the same long-time behavior.

A.3. Short-time behavior

The short-time behavior corresponds to the large-p limit. As the boundary region Γ is smooth, the propagator $G_0(\boldsymbol{x},t|\boldsymbol{x}_0)$ is close to that in the half-space with reflecting hyperplane:

$$G_0^{\rm half}(\boldsymbol{x},t|\boldsymbol{x}_0) = \frac{{\rm e}^{-|\boldsymbol{s}-\boldsymbol{s}_0|^2/(4Dt)}}{(4\pi Dt)^{(d-1)/2}}\,\frac{{\rm e}^{-(y-y_0)^2/(4Dt)} + {\rm e}^{-(y+y_0)^2/(4Dt)}}{\sqrt{4\pi Dt}},$$

where $\boldsymbol{x} = (\boldsymbol{s},y)$ and $\boldsymbol{x}_0 = (\boldsymbol{s}_0,y_0)$. Its Laplace transform reads

$$\tilde{G}_0^{\rm half}(\boldsymbol{x},p|\boldsymbol{x}_0) = \frac{(D/p)^{\nu/2}}{(2\pi)^{d/2}D}\Big(A_1^{\nu}K_{\nu}\Big(A_1\sqrt{p/D}\Big) + A_2^{\nu}K_{\nu}\Big(A_2\sqrt{p/D}\Big)\Big),$$

where $\nu = 1-d/2$, $A_1^2 = |\boldsymbol{s}-\boldsymbol{s}_0|^2 + (y-y_0)^2$, $A_2^2 = |\boldsymbol{s}-\boldsymbol{s}_0|^2 + (y+y_0)^2$, and $K_{\nu}(z)$ is the modified Bessel function of the second kind. Setting $y = y_0 = 0$, one gets

$$\tilde{G}_0^{\rm half}(\boldsymbol{s},p|\boldsymbol{s}_0) = \frac{2(D/p)^{\nu/2}}{(2\pi)^{d/2}D}\,|\boldsymbol{s}-\boldsymbol{s}_0|^\nu K_\nu\Big(|\boldsymbol{s}-\boldsymbol{s}_0|\sqrt{p/D}\Big). \tag{A.14}$$

At large p, equation (63) implies thus

$$\begin{aligned}\frac{1}{Q_p} &\approx \frac{1}{|\Gamma|}\int\limits_\Gamma \mathrm{d}\boldsymbol{s}_0 \int\limits_\Gamma \mathrm{d}\boldsymbol{s}\, D\tilde{G}_0^{\rm half}(\boldsymbol{s},p|\boldsymbol{s}_0) \\ &\approx \frac{2(D/p)^{\nu/2}}{(2\pi)^{d/2}|\Gamma|}\int\limits_\Gamma \mathrm{d}\boldsymbol{s}_0 \int\limits_\Gamma \mathrm{d}\boldsymbol{s}\,|\boldsymbol{s}-\boldsymbol{s}_0|^\nu K_\nu\Big(|\boldsymbol{s}-\boldsymbol{s}_0|\sqrt{p/D}\Big).\end{aligned}$$

As $K_\nu(z)$ decays exponentially at large z, the main contribution comes from the points $\boldsymbol{s}\approx\boldsymbol{s}_0$. One integral yields thus $|\Gamma|$. In turn, the second integral can be evaluated by replacing the target surface by a hyperplane and using the spherical coordinates:

$$\frac{1}{Q_p} \approx \frac{2(D/p)^{\nu/2}}{(2\pi)^{d/2}}\sigma_{d-1}\int\limits_0^\infty \mathrm{d}r\, r^{d-2}\, r^\nu K_\nu\Big(r\sqrt{p/D}\Big),$$

where $\sigma_{d-1} = 2\pi^{(d-1)/2}/\Gamma((d-1)/2)$ is the surface area of the unit ball in $\mathbb{R}^{d-1}$, and we extended the upper limit of integration to infinity. The last integral can be found exactly via the identity:

$$\int\limits_0^\infty \mathrm{d}z\, z^\alpha\, K_\nu(z) = 2^{\alpha-1}\Gamma\left(\frac{\alpha+\nu+1}{2}\right)\Gamma\left(\frac{\alpha-\nu+1}{2}\right).$$

After simplifications, we get simply

$$Q_p \approx \sqrt{p/D} \qquad (p\to\infty). \tag{A.15}$$

Substituting this expression into equation (67), we can invert the Laplace transform to get the short-time approximation:

$$\rho^{\rm app}(\ell,t) \approx \left(1-\frac{2\sqrt{Dt}\,|\Gamma|}{\sqrt{\pi}|\Omega|}\right)\delta(\ell) + \frac{|\Gamma|}{|\Omega|}\mathrm{erfc}\left(\frac{\ell}{\sqrt{4Dt}}\right) \quad (t\to 0). \tag{A.16}$$

Despite its approximation character, this expression is correctly normalized.

We emphasize that equation (A.15) and the consequent relation (A.16) ignore the curvature of the target, which is known to yield non-universal corrections [105]. For instance, if the target is a sphere of radius R_1, equation (68) implies $\mu_0^{(p)} \approx \sqrt{p/D} + 1/R_1$, and its substitution into equation (77) and the evaluation of the inverse Laplace transform yield the following short-time asymptotic behavior:

J. Stat. Mech. (2022) 083205

$$\rho(\ell,t) \approx \left\{1 - \frac{|\Gamma|}{|\Omega|}\left(\frac{2\sqrt{Dt}}{\sqrt{\pi}} + \frac{Dt}{R_1}\right)\right\}\delta(\ell) + \frac{|\Gamma|}{|\Omega|}\mathrm{e}^{-\ell/R_1}\left\{\left(1 - \frac{2\ell}{R_1} + \frac{\ell^2+2Dt}{2R_1^2}\right)\mathrm{erfc}\left(\frac{\ell}{\sqrt{4Dt}}\right) + \frac{(4-\ell/R_1)\sqrt{Dt}}{R_1\sqrt{\pi}}\mathrm{e}^{-\ell^2/(4Dt)}\right\}. \tag{A.17}$$

Its comparison with equation (A.16) reveals that the regular part of this expression contains in an additional factor $\mathrm{e}^{-\ell/R_1}$ due to the curvature, as well as higher-order corrections. The above expression is valid for $\sqrt{Dt} \ll R_1$. One can distinguish two regimes depending on whether ℓ is smaller or larger than $\sqrt{Dt}$. When $\sqrt{Dt} \ll \ell$, one gets in the leading-order:

$$\rho(\ell,t) \approx \left(1 - \frac{2\sqrt{Dt}\,|\Gamma|}{\sqrt{\pi}|\Omega|}\right)\delta(\ell) + \frac{2\sqrt{Dt}\,|\Gamma|}{\sqrt{\pi}\,|\Omega|\,\ell}\mathrm{e}^{-\ell^2/(4Dt)}\mathrm{e}^{-\ell/R_1}. \tag{A.18}$$

In the opposite regime $\ell \ll \sqrt{Dt}$, the probability density approaches

$$\rho(\ell,t) \approx \left(1 - \frac{2\sqrt{Dt}\,|\Gamma|}{\sqrt{\pi}|\Omega|}\right)\delta(\ell) + \frac{|\Gamma|}{|\Omega|}\left(1 + \frac{4\sqrt{Dt}}{\sqrt{\pi}R_1} + \frac{Dt}{R_1^2}\right). \tag{A.19}$$

This relation shows the limitation of the PEA (58), which predicts a different limit at short times and small ℓ. This difference is seen figure 2(a). A better understanding of the origins of this deviation presents an interesting open problem.

References

[1] Rice S 1985 *Diffusion-Limited Reactions* (Amsterdam: Elsevier)
[2] Lauffenburger D A and Linderman J 1993 *Receptors: Models for Binding, Trafficking, and Signaling* (New York: Oxford University Press)
[3] Redner S 2001 *A Guide to First Passage Processes* (Cambridge: Cambridge University Press)
[4] Schuss Z 2013 *Brownian Dynamics at Boundaries and Interfaces in Physics, Chemistry and Biology* (New York: Springer)
[5] Metzler R, Oshanin G and Redner S (ed) 2014 *First-Passage Phenomena and Their Applications* (Singapore: World Scientific)
[6] Lindenberg K, Metzler R and Oshanin G (ed) 2019 *Chemical Kinetics: Beyond the Textbook* (Singapore: World Scientific)
[7] Berg H C and Purcell E M 1977 Physics of chemoreception *Biophys. J.* **20** 193–219
[8] Weiss G H 1986 Overview of theoretical models for reaction rates *J. Stat. Phys.* **42** 3
[9] Condamin S, Bénichou O, Tejedor V, Voituriez R and Klafter J 2007 First-passage times in complex scale-invariant media *Nature* **450** 77
[10] Grebenkov D S 2007 NMR survey of reflected Brownian motion *Rev. Mod. Phys.* **79** 1077–137
[11] Bénichou O and Voituriez R 2008 Narrow-escape time problem: time needed for a particle to exit a confining domain through a small window *Phys. Rev. Lett.* **100** 168105
[12] Bénichou O, Grebenkov D, Levitz P, Loverdo C and Voituriez R 2010 Optimal reaction time for surface-mediated diffusion *Phys. Rev. Lett.* **105** 150606
[13] Bénichou O, Chevalier C, Klafter J, Meyer B and Voituriez R 2010 Geometry-controlled kinetics *Nat. Chem.* **2** 472–7

J. Stat. Mech. (2022) 083205

[14] Bénichou O, Loverdo C, Moreau M and Voituriez R 2011 Intermittent search strategies *Rev. Mod. Phys.* **83** 81–129
[15] Bressloff P C and Newby J M 2013 Stochastic models of intracellular transport *Rev. Mod. Phys.* **85** 135–96
[16] Bénichou O and Voituriez R 2014 From first-passage times of random walks in confinement to geometry-controlled kinetics *Phys. Rep.* **539** 225–84
[17] Godec A and Metzler R 2016 First passage time distribution in heterogeneity controlled kinetics: going beyond the mean first passage time *Sci. Rep.* **6** 20349
[18] Godec A and Metzler R 2016 Universal proximity effect in target search kinetics in the few-encounter limit *Phys. Rev.* X **6** 041037
[19] Grebenkov D S 2016 Universal formula for the mean first passage time in planar domains *Phys. Rev. Lett.* **117** 260201
[20] Chechkin A V, Seno F, Metzler R and Sokolov I M 2017 Brownian yet non-Gaussian diffusion: from superstatistics to subordination of diffusing diffusivities *Phys. Rev.* X **7** 021002
[21] Lanoiselée Y, Moutal N and Grebenkov D S 2018 Diffusion-limited reactions in dynamic heterogeneous media *Nat. Commun.* **9** 4398
[22] Levernier N, Dolgushev M, Bénichou O, Voituriez R and Guérin T 2019 Survival probability of stochastic processes beyond persistence exponents *Nat. Commun.* **10** 2990
[23] Szabo A, Zwanzig R and Agmon N 1988 Diffusion-controlled reactions with mobile traps *Phys. Rev. Lett.* **61** 2496–9
[24] Redner S and Krapivsky P L 1999 Capture of the lamb: diffusing predators seeking a diffusing prey *Am. J. Phys.* **67** 1277–83
[25] Bartumeus F, Catalan J, Fulco U L, Lyra M L and Viswanathan G M 2002 Optimizing the encounter rate in biological interactions: Levy versus Brownian strategies *Phys. Rev. Lett.* **88** 097901
[26] James A, Plank M J and Brown R 2008 Optimizing the encounter rate in biological interactions: ballistic versus Levy versus Brownian strategies *Phys. Rev.* E **78** 051128
[27] Oshanin G, Vasilyev O, Krapivsky P L and Klafter J 2009 Survival of an evasive prey *Proc. Natl Acad. Sci. USA* **106** 13696–701
[28] Sanders D P 2009 Exact encounter times for many random walkers on regular and complex networks *Phys. Rev.* E **80** 036119
[29] Tejedor V, Schad M, Bénichou O, Voituriez R and Metzler R 2011 Encounter distribution of two random walkers on a finite one-dimensional interval *J. Phys. A: Math. Theor.* **44** 395005
[30] Amitai A, Kupka I and Holcman D 2012 Computation of the mean first-encounter time between the ends of a polymer chain *Phys. Rev. Lett.* **109** 108302
[31] Tzou J C, Xie S and Kokolnikov T 2014 First-passage times, mobile traps, and Hopf bifurcations *Phys. Rev.* E **90** 062138
[32] Agliari E, Blumen A and Cassi D 2014 Slow encounters of particle pairs in branched structures *Phys. Rev.* E **89** 052147
[33] Agliari E, Cassi D, Cattivelli L and Sartori F 2016 Two-particle problem in comblike structures *Phys. Rev.* E **93** 052111
[34] Peng J and Agliari E 2019 First encounters on combs *Phys. Rev.* E **100** 062310
[35] Le Vot F, Yuste S B, Abad E and Grebenkov D S 2020 First-encounter time of two diffusing particles in confinement *Phys. Rev.* E **102** 032118
[36] Nayak I, Nandi A and Das D 2020 Capture of a diffusive prey by multiple predators in confined space *Phys. Rev.* E **102** 062109
[37] Le Vot F, Yuste S B, Abad E and Grebenkov D S 2022 First-encounter time of two diffusing particles in two- and three-dimensional confinement *Phys. Rev.* E **105** 044119
[38] Lévy P 1965 *Processus Stochastiques et Mouvement Brownien* (Paris: Gauthier-Villard)
[39] Ito K and McKean H P 1965 *Diffusion Processes and Their Sample Paths* (Berlin: Springer)
[40] Freidlin M 1985 *Functional Integration and Partial Differential Equations* (*Annals of Mathematics Studies*) (Princeton, NJ: Princeton University Press)
[41] Grebenkov D S 2007 Residence times and other functionals of reflected Brownian motion *Phys. Rev.* E **76** 041139
[42] Grebenkov D S 2019 Probability distribution of the boundary local time of reflected Brownian motion in Euclidean domains *Phys. Rev.* E **100** 062110
[43] Grebenkov D S 2020 Paradigm shift in diffusion-mediated surface phenomena *Phys. Rev. Lett.* **125** 078102
[44] Collins F C and Kimball G E 1949 Diffusion-controlled reaction rates *J. Colloid Sci.* **4** 425
[45] Sano H and Tachiya M 1979 Partially diffusion-controlled recombination *J. Chem. Phys.* **71** 1276

J. Stat. Mech. (2022) 083205

[46] Sano H and Tachiya M 1981 Theory of diffusion-controlled reactions on spherical surfaces and its application to reactions on micellar surfaces *J. Chem. Phys.* **75** 2870–8
[47] Shoup D and Szabo A 1982 Role of diffusion in ligand binding to macromolecules and cell-bound receptors *Biophys. J.* **40** 33–9
[48] Sapoval B 1994 General formulation of Laplacian transfer across irregular surfaces *Phys. Rev. Lett.* **73** 3314–6
[49] Filoche M and Sapoval B 1999 Can one hear the shape of an electrode? II. Theoretical study of the Laplacian transfer *Eur. Phys. J.* B **9** 755–63
[50] Bénichou O, Moreau M and Oshanin G 2000 Kinetics of stochastically gated diffusion-limited reactions and geometry of random walk trajectories *Phys. Rev.* E **61** 3388
[51] Sapoval B, Filoche M and Weibel E R 2002 Smaller is better-but not too small: a physical scale for the design of the mammalian pulmonary acinus *Proc. Natl Acad. Sci. USA* **99** 10411–6
[52] Grebenkov D S, Filoche M and Sapoval B 2003 Spectral properties of the Brownian self-transport operator *Eur. Phys. J.* B **36** 221–31
[53] Grebenkov D S, Filoche M, Sapoval B and Felici M 2005 Diffusion-reaction in branched structures: theory and application to the lung acinus *Phys. Rev. Lett.* **94** 050602
[54] Grebenkov D S, Filoche M and Sapoval B 2006 Mathematical basis for a general theory of Laplacian transport towards irregular interfaces *Phys. Rev.* E **73** 021103
[55] Grebenkov D S 2006 Partially reflected Brownian motion: a stochastic approach to transport phenomena *Focus on Probability Theory* ed L R Velle (New York: Nova Science) pp 135–69
[56] Traytak S D and Price W S 2007 Exact solution for anisotropic diffusion-controlled reactions with partially reflecting conditions *J. Chem. Phys.* **127** 184508
[57] Bressloff P C, Earnshaw B A and Ward M J 2008 Diffusion of protein receptors on a cylindrical dendritic membrane with partially absorbing traps *SIAM J. Appl. Math.* **68** 1223–46
[58] Singer A, Schuss Z, Osipov A and Holcman D 2008 Partially reflected diffusion *SIAM J. Appl. Math.* **68** 844
[59] Grebenkov D S 2010 Searching for partially reactive sites: analytical results for spherical targets *J. Chem. Phys.* **132** 034104
[60] Grebenkov D S 2010 Subdiffusion in a bounded domain with a partially absorbing-reflecting boundary *Phys. Rev.* E **81** 021128
[61] Lawley S D and Keener J P 2015 A new derivation of Robin boundary conditions through homogenization of a stochastically switching boundary *SIAM J. Appl. Dyn. Syst.* **14** 1845–67
[62] Grebenkov D S 2015 Analytical representations of the spread harmonic measure density *Phys. Rev.* E **91** 052108
[63] Grebenkov D S 2020 Surface hopping propagator: an alternative approach to diffusion-influenced reactions *Phys. Rev.* E **102** 032125
[64] Grebenkov D S 2020 Joint distribution of multiple boundary local times and related first-passage time problems with multiple targets *J. Stat. Mech.* 103205
[65] Grebenkov D S 2021 Statistics of boundary encounters by a particle diffusing outside a compact planar domain *J. Phys. A: Math. Theor.* **54** 015003
[66] Grebenkov D S 2022 An encounter-based approach for restricted diffusion with a gradient drift *J. Phys. A: Math. Theor.* **55** 045203
[67] Bressloff P C 2022 Diffusion-mediated absorption by partially-reactive targets: Brownian functionals and generalized propagators *J. Phys. A: Math. Theor.* **55** 205001
[68] Maz'ya V G, Nazakov S A and Plamenevskii B A 1985 Asymptotic expansions of the eigenvalues of boundary value problems for the Laplace operator in domains with small holes *Math. USSR. Izv* **24** 321–45
[69] Ward M J and Keller J B 1993 Strong localized perturbations of eigenvalue problems *SIAM J. Appl. Math.* **53** 770–98
[70] Kolokolnikov T, Titcombe M S and Ward M J 2005 Optimizing the fundamental Neumann eigenvalue for the Laplacian in a domain with small traps *Eur. J. Appl. Math* **16** 161
[71] Singer A, Schuss Z, Holcman D and Eisenberg R S 2006 Narrow escape, part I *J. Stat. Phys.* **122** 437–63
[72] Singer A, Schuss Z and Holcman D 2006 Narrow escape, part II: the circular disk *J. Stat. Phys.* **122** 465
[73] Singer A, Schuss Z and Holcman D 2006 Narrow escape, part III: non-smooth domains and Riemann surfaces *J. Stat. Phys.* **122** 491
[74] Pillay S, Ward M J, Peirce A and Kolokolnikov T 2010 An asymptotic analysis of the mean first passage time for narrow escape problems: part I: two-dimensional domains *Multiscale Model. Simul.* **8** 803–35
[75] Cheviakov A F, Ward M J and Straube R 2010 An asymptotic analysis of the mean first passage time for narrow escape problems: part II: the sphere *Multiscale Model. Simul.* **8** 836–70
[76] Cheviakov A F and Ward M J 2011 Optimizing the principal eigenvalue of the Laplacian in a sphere with interior traps *Math. Comput. Modelling* **53** 1394–409

J. Stat. Mech. (2022) 083205

[77] Cheviakov A F, Reimer A S and Ward M J 2012 Mathematical modeling and numerical computation of narrow escape problems *Phys. Rev.* E **85** 021131
[78] Holcman D and Schuss Z 2014 The narrow escape problem *SIAM Rev.* **56** 213–57
[79] Bressloff P C 2022 Narrow capture problem: an encounter-based approach to partially reactive targets *Phys. Rev.* E **105** 034141
[80] Chaigneau A and Grebenkov D S 2022 First-passage times to anisotropic partially reactive targets *Phys. Rev.* E **105** 054146
[81] Shoup D, Lipari G and Szabo A 1981 Diffusion-controlled bimolecular reaction rates. The effect of rotational diffusion and orientation constraints *Biophys. J.* **36** 697
[82] Grebenkov D S and Oshanin G 2017 Diffusive escape through a narrow opening: new insights into a classic problem *Phys. Chem. Chem. Phys.* **19** 2723–39
[83] Grebenkov D S, Metzler R and Oshanin G 2017 Effects of the target aspect ratio and intrinsic reactivity onto diffusive search in bounded domains *New J. Phys.* **19** 103025
[84] Grebenkov D S, Metzler R and Oshanin G 2018 Towards a full quantitative description of single-molecule reaction kinetics in biological cells *Phys. Chem. Chem. Phys.* **20** 16393–401
[85] Grebenkov D S, Metzler R and Oshanin G 2019 Full distribution of first exit times in the narrow escape problem *New J. Phys.* **21** 122001
[86] Grebenkov D S, Metzler R and Oshanin G 2021 Distribution of first-reaction times with target regions on boundaries of shell-like domains *New J. Phys.* **23** 123049
[87] Mörters P and Peres Y 2010 *Brownian Motion* (*Cambridge Series in Statistical and Probabilistic Mathematics*) (Cambridge: Cambridge University Press)
[88] Grebenkov D S and Nguyen B-T 2013 Geometrical structure of Laplacian eigenfunctions *SIAM Rev.* **55** 601–67
[89] Yuste S B, Abad E and Lindenberg K 2013 Exploration and trapping of mortal random walkers *Phys. Rev. Lett.* **110** 220603
[90] Meerson B and Redner S 2015 Mortality, redundancy, and diversity in stochastic search *Phys. Rev. Lett.* **114** 198101
[91] Grebenkov D S and Rupprecht J-F 2017 The escape problem for mortal walkers *J. Chem. Phys.* **146** 084106
[92] Arendt W, ter Elst A F M, Kennedy J B and Sauter M 2014 The Dirichlet-to-Neumann operator via hidden compactness *J. Funct. Anal.* **266** 1757–86
[93] Daners D 2014 Non-positivity of the semigroup generated by the Dirichlet-to-Neumann operator *Positivity* **18** 235–56
[94] ter Elst A F M and Ouhabaz E M 2014 Analysis of the heat kernel of the Dirichlet-to-Neumann operator *J. Funct. Anal.* **267** 4066–109
[95] Behrndt J and ter Elst A F M 2015 Dirichlet-to-Neumann maps on bounded Lipschitz domains *J. Differ. Equ.* **259** 5903–26
[96] Arendt W and ter Elst A F M 2015 The Dirichlet-to-Neumann operator on exterior domains *Potential Anal.* **43** 313–40
[97] Hassell A and Ivrii V 2017 Spectral asymptotics for the semiclassical Dirichlet to Neumann operator *J. Spectr. Theory* **7** 881–905
[98] Girouard A and Polterovich I 2017 Spectral geometry of the Steklov problem (survey article) *J. Spectr. Theory* **7** 321–59
[99] Grebenkov D S 2019 Spectral theory of imperfect diffusion-controlled reactions on heterogeneous catalytic surfaces *J. Chem. Phys.* **151** 104108
[100] van den Berg M and Davies E B 1989 Heat flow out of regions in R^m *Math. Z.* **202** 463
[101] Vandenberg M and Gilkey P B 1994 Heat content asymptotics of a Riemannian manifold with boundary *J. Funct. Anal.* **120** 48
[102] Desjardins S and Gilkey P 1994 Heat content asymptotics for operators of Laplace type with Neumann boundary conditions *Math. Z.* **215** 251–68
[103] Gilkey P 2004 *Asymptotic Formulae in Spectral Geometry* (London: Chapman and Hall)
[104] Grebenkov D S, Metzler R and Oshanin G 2020 From single-particle stochastic kinetics to macroscopic reaction rates: fastest first-passage time of N random walkers *New J. Phys.* **22** 103004
[105] Grebenkov D S 2022 Depletion of resources by a population of diffusing species *Phys. Rev.* E **105** 054402

J. Stat. Mech. (2022) 083205